

PHYTOPLANKTON

Martin T. Dokulil¹ and Christina M. Kaiblinger²

¹ *Institute for Limnology, Austrian Academy of Sciences, 5310 Mondsee, Mondseestrasse 9, Austria*

² *Am Moosbach 2B/8, 5310 Mondsee, Austria*

Motto: 'A graphic tells more than 1000 words'.

1 Introduction

Autotrophic phytoplankton is an essential quality element in lakes and large rivers. Primary producers are important in the carbon cycle and in the oxygen budget through photosynthetic processes. The accumulated biomass serves as food for other trophic levels. As an element of water quality, phytoplankton composition and biomass primarily indicates eutrophication. Eutrophication is defined as an increase in primary production due to enhanced nutrient input. Negative consequences of high eutrophication include elevated oxygen saturation and pH values during the day, often decreased transparency, lowered species diversity, production of toxic substances and a general deterioration in water quality leading to restriction in usage. Development of phytoplankton biomass in large rivers however usually depends more on flow velocity, residence time and light conditions than on nutrient availability and concentration. Grazing by zooplankton and benthic filter-feeders is important in certain reaches.

The metrics required by the European Water Framework Directive (EC-WFD) shall therefore primarily evaluate the trophic status. Similar as for the trophic concept used in lakes, additional parameters relevant to assess the trophic level are necessary. Phosphorus is assumed to be the most relevant nutrient for phytoplankton growth and hence total phosphorus (TP) is taken as the best predictor. Nitrogen concentration is needed to judge any deficiency relative to phosphorus, and chlorophyll-a is used as an additional measure of biomass. Development of diatoms can be estimated from concentration of dissolved silica. Availability of under-water light, important for photosynthesis, can be calculated from suspended solids.

Phytoplankton can also be used to estimate impacts from chloride concentration or to evaluate changes in hydromorphology which affect phytoplankton assemblages. Regulated stretches decrease retention time resulting in reduced biomass development. Impounded or artificial deepened river sections are more similar to lakes indicated by an increase in species more common in standing waters and a reduction in the contribution of benthic taxa usually common in free flowing rivers.

Within the Danube River basin phytoplankton assessment is particularly relevant because the River Danube as well as several of the larger tributaries have a great potential to produce large amounts of phytoplankton biomass. Some stretches may even carry 'true' river plankton (potamoplankton). Monitoring of phytoplankton diversity will help to assess changes in nutrient input and pollution control. The development of the nutrient levels and the associated phytoplankton biomass in the Danube River Basin finally has a large impact on the Black Sea.

2 Material and Methods

Qualitative and quantitative investigations were carried out along the Danube, its larger tributaries and side arms as part of JDS2 with the aim to evaluate their trophic status, to reveal longitudinal variations and to detect influences from the tributaries. Samples were taken in the middle of the river from the surface with a black bucket (8 L) and used for all further analysis. A qualitative sample was taken with a plankton

net (10 µm mesh size), Secchi-depth and incident PAR-radiation was measured at each sampling station. For sampling station details see Table 1, Annex A and The Factsheets.

2.1 Transparency and light measurements

Transparency was estimated from Secchi-depth using a white disk of 25 cm diameter. The disk was fixed to a stainless steel expandable pole to allow precise depth readings even when water current is high. Secchi-depth (z_{SD}) is reported as the average of three measurements done on the sunny side of the ship. Photosynthetic available radiation (PAR) in the range of 400 – 700 nm was measured above the water with a 2π flat Li-Cor sensor in units of $\mu\text{mol m}^{-2}\text{s}^{-1}$. Sub-surface PAR (E_0') was calculated from the measurements in air assuming 10% reflection. Under-water PAR (E_z) was derived from an independent calibration of light measurements versus z_{SD} (on average 25% E_0' at Secchi-depth). This information was used to calculate the vertical attenuation coefficient (K), see formula 1 below and the depth of the euphotic zone (z_{eu} per definition equal to 1% L.I.): As an independent estimate, z_{eu} was assumed to be equal to $3 \times z_{SD}$ (REYNOLDS 1984, p. 147).

$$(1) \quad K = (\ln E_0' - \ln E_z)/z$$

with E_0' = subsurface PAR, E_z = PAR at depth z , and z = depth in meters

2.2 Determination of suspended solids

Suspended solids (SS) were immediately separated by filtering an aliquot, 0.2 - 1 L onto pre-combusted and pre-weighed glass fiber filters (GF/F) for gravimetric analysis (GREENBERG et al. 2005). The filters were pre-dried on board in an oven at 35°C and kept in a desiccator for final analysis in the laboratory. After drying the filters at 105°C for 4 hours, total suspended solids (TSS) was calculated from the difference in dry weight between the filter plus residue and the blank filter. The filter was then combusted in a muffle furnace at 500°C for 4 hours. Ash-free dry weight of inorganic suspended solids (ISS) was determined again from the difference in weight to the blank filter. The difference in the weight before and after ignition is assumed to be roughly equivalent to organic substances (OSS). All results for SS are given as mg L^{-1} .

2.3 Chlorophyll-a and pigment analysis

On-board analysis included the immediate *in vivo* measurement of photosynthetic pigments by delayed fluorescence (DF) with two different instruments (KRAUSE et al. 1982, GERHARDT and BODEMER 1999).

In the DF-kinetic photometer, 'photosynthetic active' chlorophyll-a from the P680 reaction centre is estimated from the fluorescence decay curve in the dark following a strong light pulse (DFK). Results are directly proportional to the quanta absorbed and therefore provide an estimate of physiological acclimation to environmental conditions. Measurements are sensitive over a wide range (0.2 - 1000 mg L^{-1} Chl-a). Values are reported here as the average and standard deviation of three measurements.

An advanced application is DF spectroscopy (DFS) which detects algal groups from pigment composition (Cyanobacteria, Cryptophyta, Bacillariophyceae inclusive Chrysophyceae and Dinophyta and Chlorophyceae inclusive Euglenophytes and Conjugatophyceae). The algal assemblage is exposed to monochromatic light between 400-700 nm and the resulting DF spectrum recorded (GERHARDT and BODEMER 1998). Concentration of algal groups is calculated from calibration curves by a deconvolution program and reported as chl-a equivalents. For a more detailed description of both techniques refer to the Annex D and the references therein.

Total chlorophyll-a and phaeopigment concentration is analyzed using the hot extraction technique (ISO 10 260). An aliquot, 0.2 to 2 liters according to the phytoplankton abundance, is filtered onto GF/C filters, stored at -35°C and extracted and analyzed with a week in the laboratory. Extinction is measured at the red

peak of chlorophyll-a at 665 nm corrected for background absorption using the extinction 750 nm before and after acidification. From these measurements, chlorophyll-a and phaeopigment concentration is calculated. Additional extinction measurements are made in the ethanol extracts at 510, 480, and 430 nm. Margalef's pigment ratio is calculated from E_{430}/E_{665} as an estimator of algal growth and development (MARGALEF 1960, 1964). Total carotenoid concentration is estimated from background corrected extinctions at 480 and 510 nm according to PARSONS et al. (1984). Further methodological and calculation details are included in Annex E.

2.4 Phytoplankton Analyses

Qualitative samples were taken with a 10 μm plankton net which has an opening diameter of 12 cm and is 1m long (Fa. UWITEC). Algae were largely determined on board using the unpreserved concentrated net-samples. Sub-samples preserved with formalin were evaluated for diatom species by the acid-combustion technique. The general system and the determination of particular taxa in the qualitative investigation of phytoplankton are based the monographs and studies cited in chapter 4.5.8 References used for algal identification

Quantitative samples (100 ml) for phytoplankton counting and sizing were fixed with 0.4 ml Utermöhl's acetic acid Lugol solution (Tab. 1), preserved with a few drops of formalin in brown screw cap glass bottles and stored in a cool dry place (EN 15204, PADISÁK et al., 1999).

Table 1 Acid and alkaline version of Utermöhl's Lugol solution

1. Dissolve 20g KI in 200 ml of distilled water
2. Dissolve 10g crystalline iodine
3. Add 20 ml of glacial acetic acid or 10g Sodium-Acetate ($\text{CH}_3\text{COO-Na}$)

The solution can be stored in a brown glass bottle at room temperature for at least 1 year.

Samples were processed in the laboratory applying the sedimentation technique (UTERMÖHL 1958). Depending on concentration, samples of 1 to 30 ml were settled for 24 hours in sedimentation chambers. In cases of very high turbidity and when only small amounts could be settled, more than one chamber was counted. Enumeration was done on a NIKON inverted microscope. Counts were stored and processed electronically using the computer software Opticount V 08/2001. Smaller organisms were enumerated from transects or fields at high magnification (objectives 40x or 60x). Abundance of the larger taxa was estimated from counts of at least half the chamber bottom using objectives 10x or 20x. At least 100 individuals of the more important taxa present were counted or at least 400 individuals per sample resulting in a counting error of less than 10% per sample or <20% per taxon (LUND et al. 1958). The number counted was converted into population density (unit cells L^{-1}). Population density was converted to biovolume using specific cell volumes of each taxon. Size class specific cell volume was derived from recommended shapes (HILLEBRAND et al. 1999). The appropriate linear dimensions were measured on at least 25 randomly selected individuals with the image analysis system Lucia V 3.51. The volume of each of the measured cells was calculated and then averaged to obtain mean cell volume (SMAYDA 1978). If linear dimensions are measured in μm , cell volume is given in μm^3 for each taxon or operational unit. Total biovolume of the assemblage is then calculated from:

$$(2) \quad B = \sum (b_i * N_i = b_1 * N_1 + b_2 * N_2 + \dots b_s * N_s)$$

with B = total biovolume in $\mu\text{m}^3 \text{ L}^{-1}$
 S = number of species in the sample ($i = 1, 2, \dots s$)
 b_i = cell volume of species i in μm^3
 N_i = abundance of species i as number of individuals L^{-1}

Conversion from biovolume to fresh-weight biomass assumes a mean specific density of 1. Average cell biomass is then given in pg (10^{-12} g).

The following relations apply:

$$\begin{aligned} 10^9 \mu\text{m}^3 &= 1 \text{ mg} \\ 10^6 \mu\text{m}^3 &= 1 \mu\text{g} \\ 10^3 \mu\text{m}^3 &= 1 \text{ ng} \end{aligned}$$

$$\begin{aligned} 10^6 \mu\text{m}^3 \text{ L}^{-1} &= 1 \mu\text{g L}^{-1} \\ 1 \text{ mm}^3 \text{ L}^{-1} &= 1 \text{ mg L}^{-1} \\ 1 \text{ cm}^3 \text{ m}^{-3} &= 1 \text{ g m}^{-3} = \text{mg L}^{-1} \end{aligned}$$

Fresh-weight biomass is usually given as integer values in $\mu\text{g L}^{-1}$. Details can be found in Annex G.

2.5 Photosynthetic parameters of phytoplankton (FRRF)

Active fluorescence measurements were acquired from water surface samples at 96 locations (78 from the Danube and 18 from tributaries) in a black plastic bucket which was protected against ambient light using a commercial available Fast Repetition Rate (FRR)-Fluorometer (Fasttracka, Chelsea Instruments Co Ltd.). Baseline, scatter and reference calibration were carried out following the user manual. The instrument response function was calibrated for gain 0, 1, 4 and 16. Blanks were determined for the light and the dark chamber using GF/C filtered Danube water at each single location. The acquisition protocol was set to provide 100 saturation flashes per sequence with a saturation flash duration of approximately 1.5 μs , spaced 15 μs apart, followed by 20 relaxation flashes ($\sim 1.1 \mu\text{s}$ duration, 80 μs apart). The sleeptime between acquisition pairs was set to 50 ms. On each sampling location, at least one, in most cases 3 replicats were taken, providing 30 pairs of measurements each. From the controlled data, arithmetic means and standard deviations for each sampling location were calculated. The initial fluorescence (F_0), the maximum fluorescence (F_m) and the functional absorption cross section of PSII (σ_{PSII}) were derived using the biophysical model of KOLBER et al. (1998). The quantum efficiency of PSII was calculated from variable fluorescence ($F_v = F_m - F_0$) normalised to F_m , indicating the proportion of functional PSII reaction centres (GEIDER et al. 1993, KOLBER and FALKOWSKI 1993). Fluorescence-based productivity was calculated following the model of KOLBER and FALKOWSKI (1993) which qualitatively predicts photosynthetic rates from changes in the quantum yield of fluorescence:

$$(3) \quad P_{\text{FRRF}} = E \sigma_{\text{PSII}} q_p f \eta_{\text{PSII}} (3600/4) M_C / M_{\text{Chla}} A$$

A is a factor containing the conversion-factors from quanta to mol photons for irradiance, and m^2 to \AA for σ_{PSII} . The term (3600/4) stands for the calculation from seconds to hours (3600), and 4 electrons, which are required to fix 1 molecule of carbon (1/4).

Table 2 Notation of fluorescence–photosynthesis relationship

F_0	In vivo fluorescence measured in dark adapted state when all reaction centres are open
F_m	In vivo fluorescence following a saturation flash, all reaction centres are closed
F_v	Variable fluorescence [$F_v = F_m - F_0$]
PSII	Photosystem II
P_{FRRF}	Fluorescence based Productivity [$\text{mg C mg Chla}^{-1} \text{ h}^{-1}$]
E	Irradiance [$\text{mol Photons m}^{-2} \text{ s}^{-1}$]
σ_{PSII}	Functional absorption cross-section of PSII [$\text{m}^2 \text{ quanta}^{-1}$]
q_p	Photochemical quenching
η_{PSII}	Ratio of PSII reaction centres to Chl-a ($=4n_{\text{O}_2}$) [$\text{mol electrons mol Chla}^{-1}$]
M_C/M_{Chla}	Molecular masses of carbon and chlorophyll-a

Details on active fluorescence measurements and technical details of the instrument used can be obtained from Annex F.

2.6 Graphical and statistical analysis

Basic data are collected and calculated in Microsoft Excel spreadsheets which are also used for storage, preliminary plotting, and databanks. Graphics are presented mainly using Sigmaplot for Windows, Version 10.0 (Systat Software 2006). Data were log-transformed before performing statistical analysis using SigmaStat for Windows, Version 3.5 (Systat Software 2006).

3 Results

3.1 Physical and chemical factors

Essential prerequisites for the growth of phytoplankton are water temperature, under-water light availability and support of essential macro-nutrients. The data reported here were largely obtained on board during the cruise and several of them are kindly provided by Carmen Hamchevichi.

Variation in water temperature is moderate during the observation period (Figure 5B). Average surface water temperature (SWT) in the middle of the river is 21°C (range 17.4 – 24.9). In the upper reaches temperature increase significantly from 17.4°C at river rkm 2600, upstream of Iller to the highest value of 24.9°C at Szob in Hungary, rkm 1707 ($r^2 = 0.44$, $n = 21$, $p < 0.001$). For the remaining part of the river, water temperature tends to decrease ($r^2 = 0.30$, $n = 56$, $p < 0.001$). Most of the variation in SWT as well as the tendencies are simply a reflection of the weather conditions and the late summer/early fall period of the year. In general, water temperature is sufficiently high to support algal growth, particularly for green algal development.

Availability of light depends on the amount of incoming radiation from the sun and attenuation under-water which is largely determined by total suspended solids (TSS). Photosynthetic available radiation at mid-day (11 to 14 hours) varies widely from 165 $\mu\text{mol m}^{-2} \text{s}^{-1}$ to 2859 $\mu\text{mol m}^{-2} \text{s}^{-1}$ (median 950 $\mu\text{mol m}^{-2} \text{s}^{-1}$) depending on weather conditions, particularly cloudiness. Highest values are observed in August in the upper reach when sunny conditions prevailed (Figure 1A).

Secchi-depth (SD), as a simple measure of visibility, reflects the turbidity of the water, in the case of the River Danube and its tributaries largely a result of inorganic suspended particles (Figure 1B). Visibility varies between 0.2 m in the St. Gheorge arm of the Danube Delta (rkm 94) and 1.65 m in the Iron Gate II impoundment (rkm 865), mean 0.9 m. Suspended solids also determine the extent of the euphotic zone (z_{eu}), defined as the depth where surface light intensity is reduced to 1% (Figure 1B). This is the zone where positive rates of photosynthesis occur ranging from 0.7 m to 5.5 m (mean 3.0 m). Under-water light conditions are summarized by the vertical attenuation coefficient which ranges from 0.8 m^{-1} to 6.9 m^{-1} (Fig. 1C). Statistics of these and further variables can be found in Table 1.

Table 3 Summary of descriptive statistics for physical variables in the River Danube during JDS2

	Size	Mean	C.I. Mean	Min	Max	Median
Secchi-depth [m]	77	0.9	0.08	0.2	1.7	0.9
PAR [$\mu\text{mol m}^{-2} \text{s}^{-1}$]	77	582	115	20	2800	415
Attenuation coefficient, K [ln m^{-1}]	77	1.96	0.29	0.84	6.93	1.54
Euphotic depth, Z_{eu} [m]	77	3.0	0.3	0.7	5.5	3.0
Total suspended solids, TSS [mg L^{-1}]	77	19.4	4.1	3.9	87.6	13.4
Inorganic particles ISS [mg L^{-1}]	77	15.8	3.7	2.5	77.6	9.6
Ignition loss, OSS [mg L^{-1}]	77	3.6	0.5	1.2	12.4	3.0

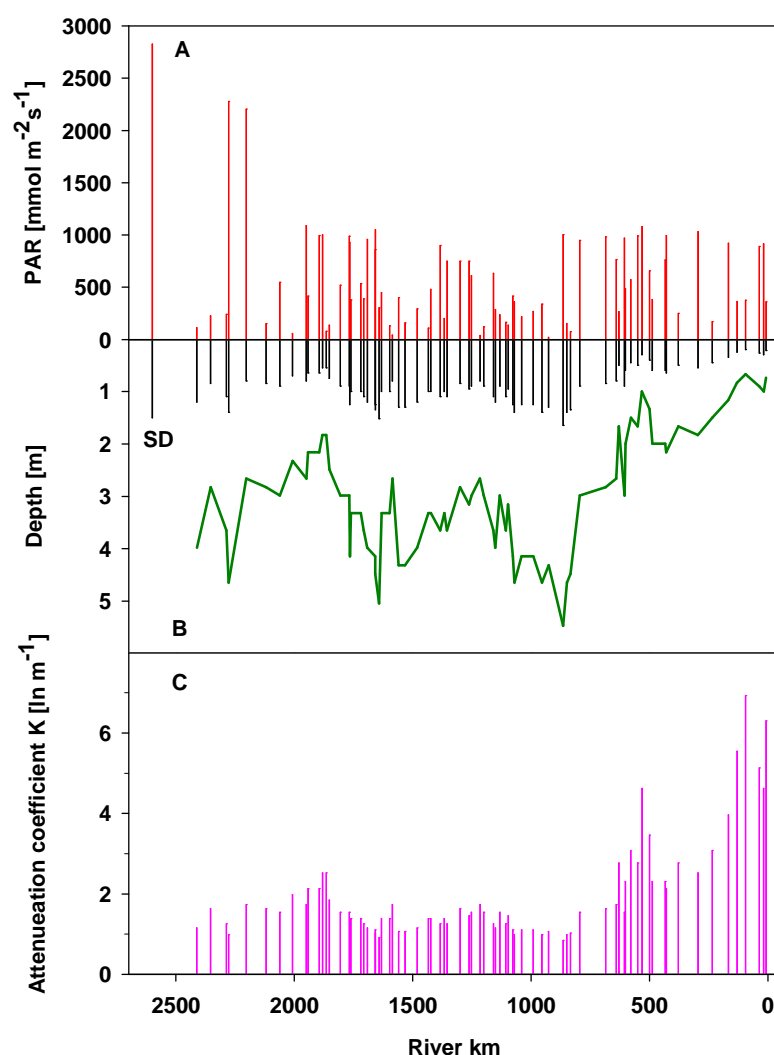


Fig. 1 Physical variables in the River Danube during JDS2. A. Photosynthetic active radiation (PAR) above the water in units of $\mu\text{mol photons m}^{-2} \text{ s}^{-1}$. B. Secchi-depth visibility in meters and the depth of euphotic zone (z_{eu}) in meters (green line). C. Attenuation coefficient (K) in units of $\ln \text{ m}^{-1}$.

Total suspended solids (TSS) are low, $4.6\text{--}7.0 \text{ mg L}^{-1}$ in the German stretch. After the confluence with the river Inn ($\text{TSS } 31.7 \text{ mg L}^{-1}$), turbidity increases and remains moderately high throughout the Austrian part (Fig. 2). A first peak of 30.5 mg L^{-1} is recorded at Bratislava (SK) after the confluence with the River Morava (114.8 mg L^{-1}). The high values there are a reflection of the high discharge during the observation period. TSS remains low or moderate ($3.9\text{--}18.0 \text{ mg L}^{-1}$) thereafter until Novi Sad (RS) where a second peak of around 20 mg L^{-1} occurs. The rivers Tisa and Sava further dilute TSS which remains low to moderate (average 9.7 mg L^{-1} until the rivers Iskar and Olt bring in loads of suspended solids. From rkm 602 onwards, TSS steadily increases towards the outflow to the Black Sea (87.6 mg L^{-1}). The increase is mainly due to inorganic suspended solids washed in from the large tributaries. Organic suspended solids (OSS), derived from loss on ignition, are low with an average of 4.5 mg L^{-1} ($\approx 25\%$ of TSS) and a peak of 12.4 mg L^{-1} at Novi Sad (RS). High contribution from organic substances is found in the tributaries, particularly Arges (83%) and Timok (76%) but also downstream of Novi Sad (61%).

The concentration of the TSS is related to Secchi disk visibility (Fig.2). These two variables are significantly correlated ($r^2 = 0.75$, $n = 96$, $p < 0.001$) as shown in Fig 3. Similarly, the attenuation coefficient k of the under-water light is strongly correlated with both TSS and ISS (Fig. 4). Somewhat weaker but still significant, k is correlated to OSS (Fig 4C).

A comparison of z_{eu} from Fig. 1B with total water column depth however reveals that large parts of the river Danube may not have a positive production balance (Fig. 5A). This situation is somehow also reflected in the saturation values of dissolved oxygen (DO%). The upper- and lower reaches, from upstream Iller to Baja and below Kozloduy (rkm 685) vary around saturation level (100%) except for some under-saturated side-arms. From Baja onwards until rkm 1216, upstream of the Tisa, DO is supersaturated peaking downstream of Novi Sad (114.5%), corresponding with maximum biomass development. After the confluent with the River Tisa, the oxygen content drops to less than 40% and remains moderately low between 80 and 90% until Calafat, rkm 795. Not surprisingly, this is also the region where ammonium concentrations are highest peaking in the Iron Gate Reservoir (Fig. 5C). Soluble reactive phosphorus (SRP), also called ortho-phosphate ($PO_4\text{-P}$) is never limiting (average $36 \mu\text{g L}^{-1}$, range 10-93). Again the region of maximum biomass development coincides with rapid declining SRP concentrations (Fig. 5D). Dissolved silica is slightly declining from up- to downstream but is never limiting diatom growth.

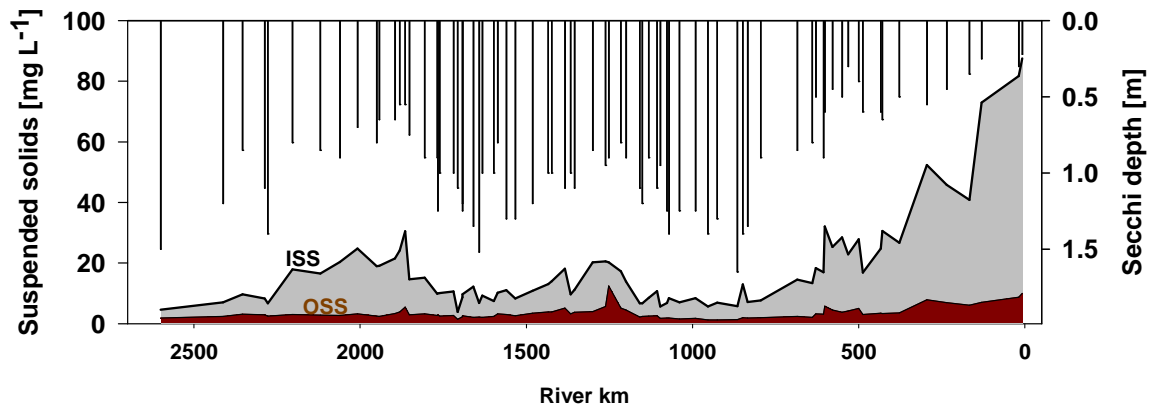


Fig. 2 Suspended solids in the River Danube during JDS2. Inorganic suspended solids (ISS) in gray and organic suspended solids (OSS) as dark red area. Total suspended solids (TSS) are the sum of ISS and OSS. For comparison SD in meters is plotted here again as a blow up from Fig. 1B.

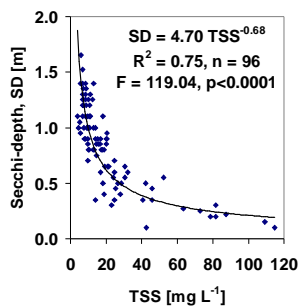


Fig. 3 Relation of Secchi-depth (SD) to total suspended solids (TSS). The hyperbolic regression curve, the equation, the number of observations, statistics and the coefficient of determination r^2 is inserted.

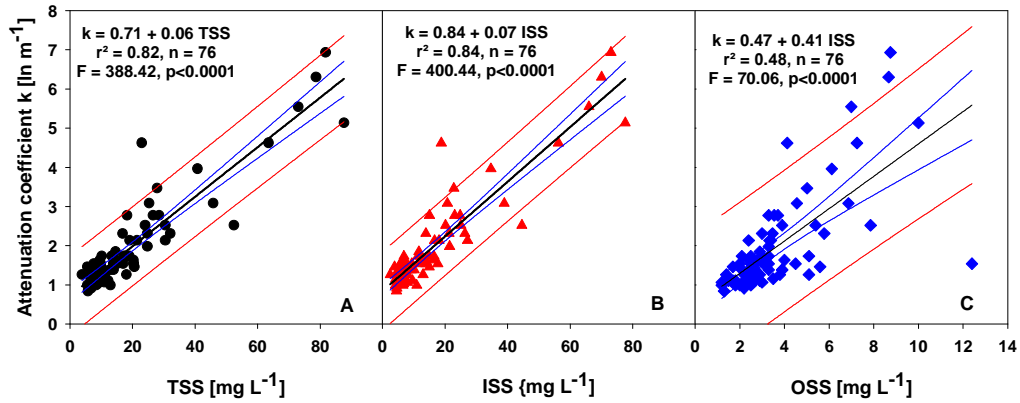


Fig. 4 Attenuation coefficient K versus: A. TSS, B. ISS, C. OSS. All in mg L^{-1} in the River Danube during JDS2. Note the different scale on the x-axis in C. The 95% confidence interval of the linear regression and the prediction interval is given as blue and red lines respectively. The linear regression equation, number of observations, statistics and the coefficient of determination r^2 is inserted in each panel.

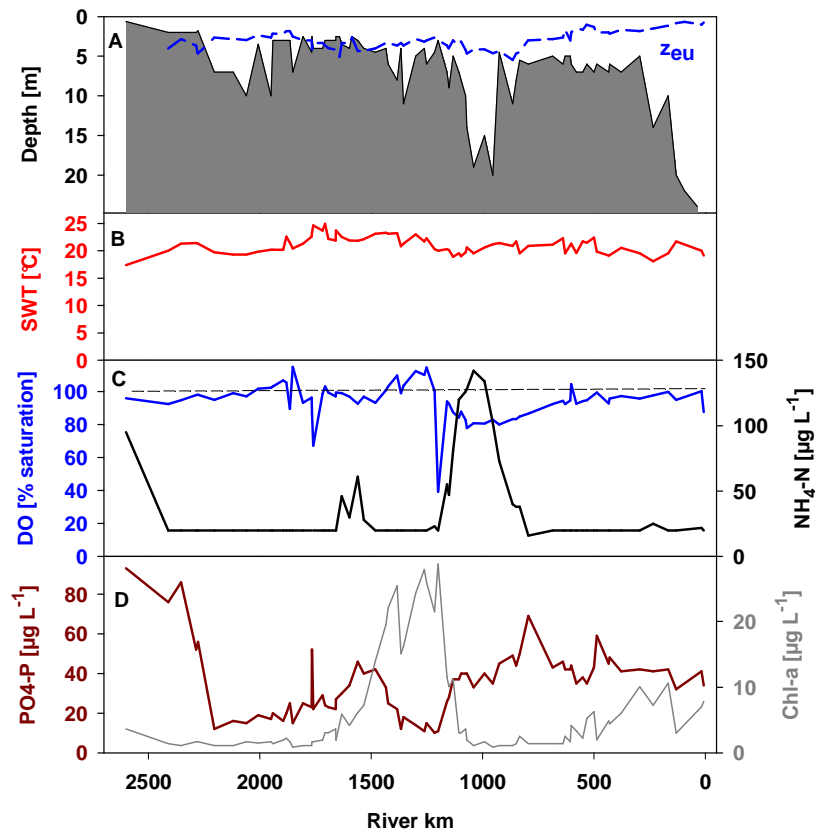


Fig. 5 A. Euphotic depth (dotted blue line) compared to the water depth of the River Danube light gray area. B. Surface water temperature (SWT), °C. C. Dissolved oxygen as % saturation (dashed line = 100%) and ammonia concentration ($\text{NH}_4\text{-N}$, $\mu\text{g L}^{-1}$). C. SRP concentration ($\text{PO}_4\text{-P}$, $\mu\text{g L}^{-1}$) and, for comparison chlorophyll-a concentration as grey line.

3.2 Chlorophyll-a and photosynthetic pigments

Concentration of **active chlorophyll-a** from open reaction centers is estimated *in vivo* from delayed fluorescence kinetics (DFK) immediately after sample collection. These measurements are directly comparable with chlorophyll-a concentrations from JDS1 because exactly the same machine was used during the first cruise. Average concentration with standard deviation is depicted for the river and the tributaries in Fig. 6. Average active chlorophyll-a is $3.2 \pm 0.4 \mu\text{g L}^{-1}$ (range 0.2 – 16.8) in the main channel and $9.8 \pm 1.0 \mu\text{g L}^{-1}$ (range 0.05 – 30.1) in the tributaries. Absolute values are in generally lower than those derived from extraction measurements of chlorophyll-a because of acclimation to light of the phytoplankton assemblage. Measurements are used for direct comparison to photosynthetic rates (see sub-chapter 5.4.3.6) but can also be used to assess the quality of the ISO extraction technique. DF-concentrations should always be lower than ISO-estimates. When comparing these two independent estimates however, 15 of the kinetic values are higher than chlorophyll-a concentrations after extraction (average 59%, range 8 – 175). This can be due to filtration and/or storage artifacts in the ISO-technique modified for the cruise (see the method section and the recommendations). Long filtration times due to suspended solids or the storage and transport of frozen samples can result in degradation of chlorophyll-a to phaeopigments which appear then in the ISO-calculations. In fact, when ISO-phaeopigment estimates are added to ISO-chlorophyll to obtain **total uncorrected chlorophyll-a** concentrations, kinetic measurements are well below total pigment estimates (average 36%, range 2 – 100). The relationship of both variables is highly significant ($r^2 = 0.83$, Fig. 7A). For more details on rational, methodology and performance of delayed fluorescence kinetics refer to Annex D.

Contribution of **major algal groups** is calculated as relative chlorophyll-a equivalents from delayed fluorescence spectroscopy (DFS) done immediately on board of the laboratory ship Argus. Results are shown in Fig. 8 for both the river Danube and the tributaries. Bacillariophyceae (diatoms) are clearly dominating at all stations in the Danube (average 59%, range 35 – 76). Higher contributions of green algae (Chlorophyta) are observed in the German stretch (37 – 63%). For the major part of the river, green algae contribute on average 25% to total chlorophyll-a (range 0 – 64%). The small flagellated species of the Cryptophyta are present at all stations in the river (mean 16%, range 0 – 47%) with higher importance in the upper reach (Austria, Slovakia, northern part of Hungary and in the Iron Gate section). Cyanoprokaryota (Cyanobacteria) are of no importance in the river and do not show up in Fig. 8, lower panel. In contrast, some of the tributaries carry large amounts of Cyanobacteria, especially the Arges which contains 80% blue-greens - exclusively species from one genus, the colonial *Microcystis*. Green algae dominate the river Timok (87%) and are an important component in most of the tributaries, particularly Sio, Hron and Ipoly. Cryptophyta are of minor importance in the streams except in the Tisa where this group contributes 36%. Chlorophyll-a concentrations from the DFS are in close agreement with ISO-determination (average 88%) and highly significant correlated (Fig. 7B, $r^2 = 0.71$). For more details on rational, methodology and performance of DFS refer to Annex E.

Chlorophyll-a and phaeopigments determined according to ISO are depicted in Fig. 9A. Chlorophyll-a concentration remains at low levels in the upstream and downstream section of the Danube. Values higher than $10 \mu\text{g L}^{-1}$ chl-a occur between Baja (HU, rkm 1481) and Grocka (RS, rkm 1132). These concentration thresholds are reached or slightly exceeded at certain points further downstream, e.g. upstream of Cernavoda, near Braila and in the Sulina canal, all in RO. Highest concentrations of around $28 \mu\text{g L}^{-1}$ chl-a are reached in the Novi Sad/Tisa confluence region between rkm 1262 and rkm 1200. Chlorophyll-a input from the tributaries (mean $14.5 \mu\text{g L}^{-1}$) varies between $0.6 \mu\text{g L}^{-1}$ from Jantra to $89.3 \mu\text{g L}^{-1}$ from Arges (Fig. 9A, bars). Phaeopigment concentration in the river follows the same pattern as chl-a, peaking downstream of Novi Sad (Fig. 9B). The share of phaeopigment to total pigment averages 36% (range 2 – 86). Greatest input of degraded pigments comes from the Velika Morava ($23.5 \mu\text{g L}^{-1}$) while only $0.3 \mu\text{g L}^{-1}$ are washed in from the Inn.

Total carotenoids (TC), a major component of the accessory pigments in phytoplankton, closely resemble the longitudinal distribution of chlorophyll-a (Fig. 9C) indicating concurrent adaptation of the photosynthetic apparatus under optimal conditions. Relatively high concentrations of $13.8 - 16.5 \mu\text{g L}^{-1}$ TC occur in the mouth of the rivers Sio, Velika Morava and Arges.

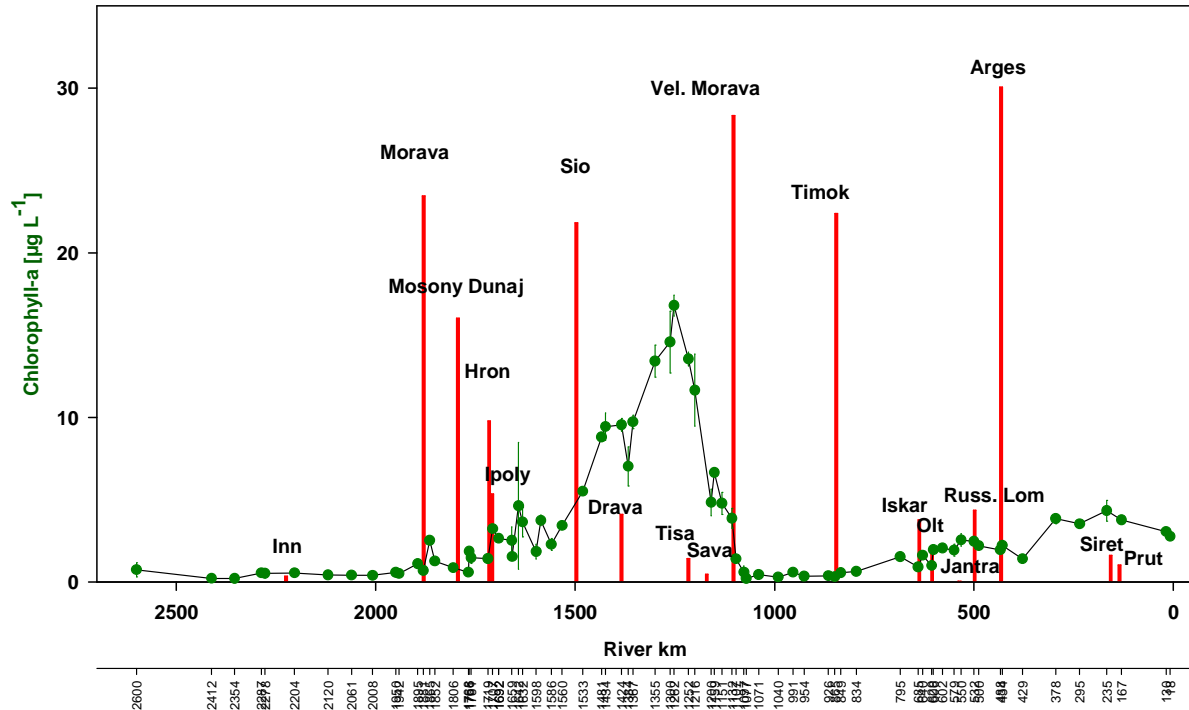


Fig. 6. Longitudinal variation of Chlorophyll-a concentration as $\mu\text{g L}^{-1}$ from delayed fluorescence kinetics (DFK) for the River Danube (green symbols and line), vertical green lines indicate standard deviation and the inlets of the major tributaries (red bars). The tributaries are named. The second x-axis gives the exact river rkm where samples are taken.

The pigment ratio, introduced by Margalef (1960) and shown in Fig. 9D, is supposed to be an indicator of the physiological status of the phytoplankton assemblage. Lower values indicate higher productivity and efficiency while higher ratios tend to be associated with lower productivity and efficiency. In general, ratios between 2 and 3 are indicative for diatom dominated plankton. The high ratio at Bratislava (SK, rkm 1865) declines thereafter until Baja (HU) indicating an increase in overall efficiency consistent with the increase in chlorophyll-a (comp. Fig. 9A). Ratios are somewhat inconclusive when biomass peaks. High ratios occur again upstream of Pancevo (RS, rkm 1159) associated with strongly decreased biomass and between river rkm 600 and 488, section Olt to Ruse, a section of slightly higher but variable chl-a values. Descriptive statistics are summarized for all pigment-related data in Table 4.

Table 4 Descriptive statistics for pigment data

In $\mu\text{g L}^{-1}$ if not otherwise specified	Size	Mean	C.I. Mean	Min	Max	Median
DF-Spectrometry (population analysis)	75	5.8	1.6	0.7	30.6	3.2
DF Kinetic	75	3.2	0.8	0.2	16.8	1.9
Total Pigment (chl-a + phaeo)	75	9.0	2.2	1.4	38.7	5.3
Chl-a ISO	75	6.2	1.7	0.8	28.8	3.1
Phaeo ISO	75	2.8	0.6	0.08	12.5	1.9
Tot Pigment Tributaries	19	19.4	12.0	1.6	91.2	10.7
Chl-a ISO Tributaries	19	14.5	10.7	0.5	89.3	6.7
Phaeo ISO Tributaries	19	4.9	2.6	0.3	23.4	3.0
% Phaeo ISO	75	36.1	3.3	4.8	72.9	34.1
% Phaeo Tributaries	19	36.5	8.6	2.0	68.7	38.3
Pigment ratio E_{430}/E_{665}	75	2.2	0.07	1.6	3.0	2.1
Total Carotenoids	75	2.2	0.6	0.3	10.0	1.2
Pigment ratio E_{430}/E_{665} Tributaries	19	2.	0.2	1.6	3.1	2.1
Total Carotenoids Tributaries	19	4.8	2.4	0.3	16.5	2.8

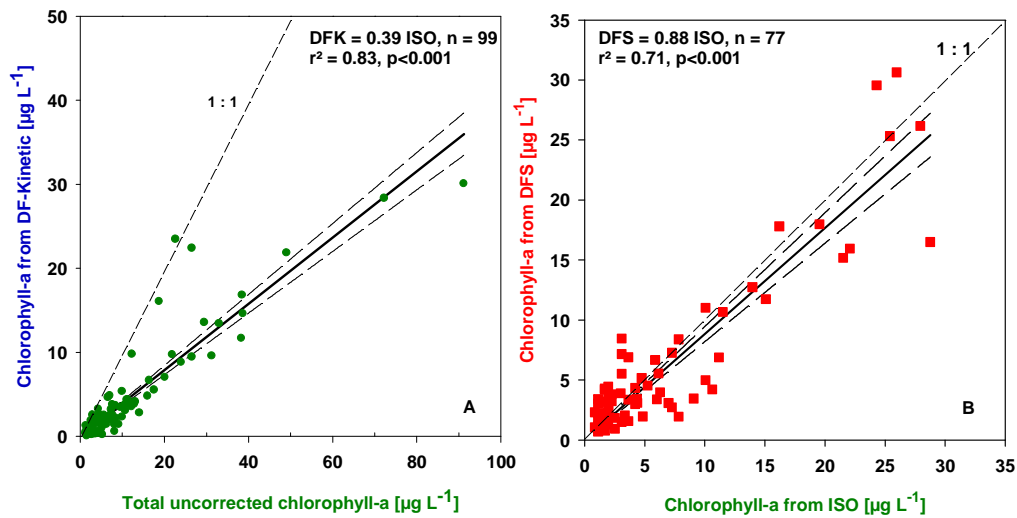


Fig. 7. A. Chlorophyll-a concentration from delayed fluorescence kinetics (DFK) related to total chlorophyll-a from ISO analysis both as $\mu\text{g L}^{-1}$ uncorrected for phaeopigments (see text for further explanation). B. Chlorophyll-a from delayed fluorescence spectroscopy (DFS) versus chl-a concentration from ISO-determination.

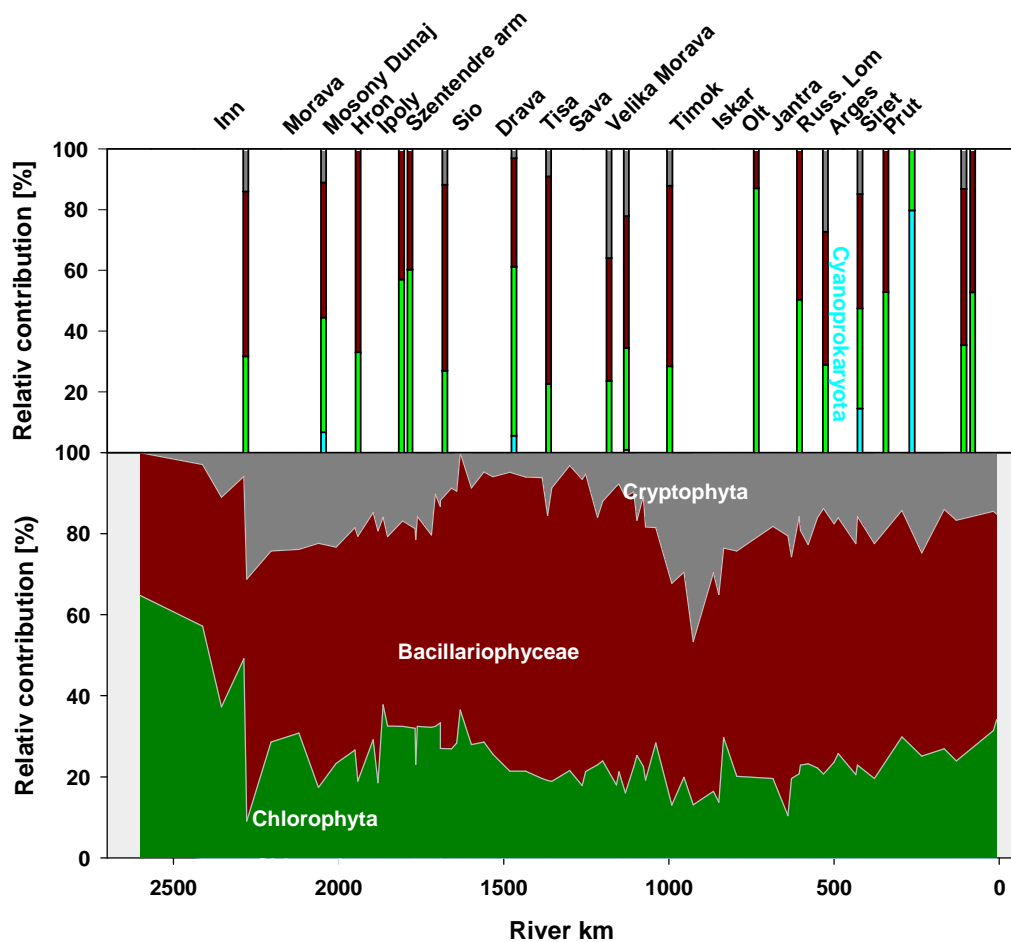


Fig. 8 Contribution of the four major algal groups Cyanoprokaryota (cyan), Cryptophyta (grey), Bacillariophyceae (dark red) and Chlorophyta (dark green) to total chlorophyll-a from delayed fluorescence spectroscopy (DFS) for the river (lower panel) and the tributaries (upper panel).

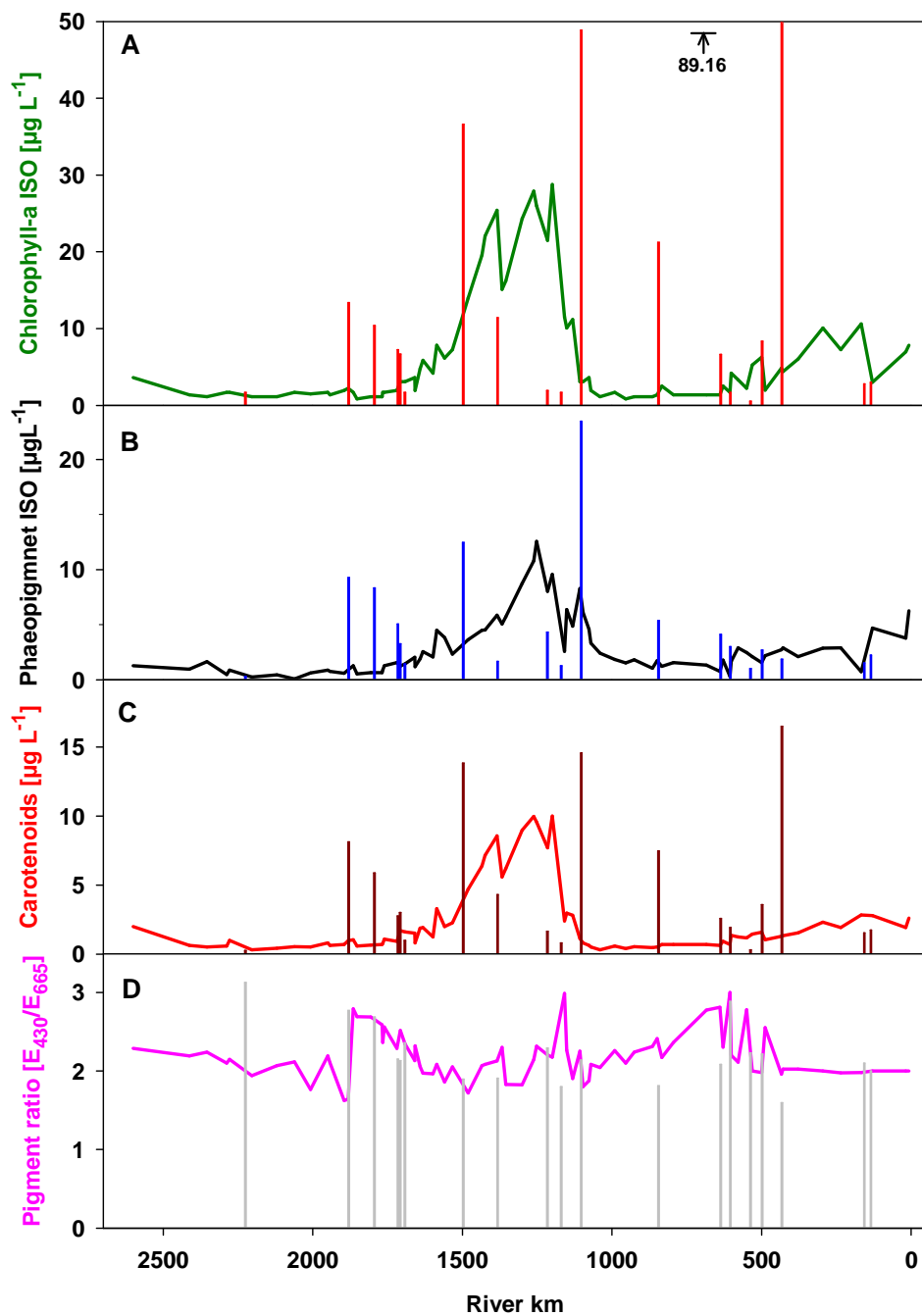


Fig. 9 Longitudinal distribution of pigment-related parameters in the river (continuous lines) and the tributaries (bars). A. Chlorophyll-a concentration of ISO-determinations. B. Phaeopigment concentration from ISO determinations. C. Total Carotenoids estimated from additional wavelength measurements in the extracts (see method section for explanation). D. Pigment ratio E_{430}/E_{665} according to Margalef as a measure of the physiological state (for further explanation see methods and the text).

3.3 Phytoplankton composition

During the JDS2 cruise, 327 algal taxa were identified in the plankton of the Danube, the side arms and the main tributaries exceeding the 261 species found during JDS1 (Table 4). Considering the plasticity in the e.g. genus *Scenedesmus* (TRAINOR 1998) no attempt has been made to identify each specimen of the green algae because we believe that many ‘species’ or ‘forms’ are just plastic varieties of species. Annex B contains the complete list of taxa and where they are found. Note that not all stations have been analyzed qualitatively.

Table 5 List of phytoplankton taxa identified during JDS2

Cyanoprokaryota

Chroococcales

Aphanocapsa holsatica
Aphanocapsa incerta
Chroococcus limneticus
Merismopedia punctata
Microcystis aeruginosa
Microcystis flos-aquae
Microcystis firma
Microstis incerta
Planktomyces bekeffii
Synechococcus ambiguus

Nostocales

Anabaena solitaria f. planktonica
Anabaena spiroides
Anabaena sp.
Aphanizomenon elenkinii
Aphanizomenon issatschenkoi
Cylindrospermopsis raciborskii
Lyngbya cf. *limnetica*.
Phormidium cf. *Mucicola*.
Planktothrix sp.
Planktothrix rubescens
Pseudanabaena catenata

Cryptophyta

Cryptomonas ovata
Cryptomonas erosa
Cryptomonas rostratiformis
Cryptomonas lens
Cryptomonas marssonii
Plagioselmis (*Rhodomonas*) *lacustris*

Xanthophyta

Dichotomococcus curvatus
Goniochloris mutica
Pseudostaurastrum hastatum
Pseudotetraedron neglectum

Dinophyta

Ceratium hirundinella furcoides
Gymnodinium sp. small
Gymnodinium helveticum
Gymnodinium uberimum
Peridinium sp.
Peridinium sp. small

Euglenophyta

Euglena oxyuris
Euglena acus
Euglena proxima
Euglena viridis
Lepocinclis fusiformis
Strombomonas fluviatilis
Phacus orbicularis
Phacus agilis var. *agilis*
Phacus pyrum var. *pyrum*

Heterokontophyta

Chrysophyceae

Chrysococcus spp.
Dinobryon sociale
Kephyrion sp.
Mallomonas acaroides und sp.

Bacillariophyceae

Centrales

Acanthoceras zachariasii
Actinocyclus normanii Morphotyp subsalsus
Aulacoseira alpigena
Aulacoseira ambigua
Aulacoseira granulata
Aulacoseira islandica var. *helvetica*
Aulacoseira subarctica
Cyclostephanos dubius
Cyclostephanos invisitatus
Cyclotella atomus
Cyclotella cyclopuncta
Cyclotella glomerata
Cyclotella krammeri
Cyclotella meneghiniana
Cyclotella ocellata
Cyclotella pseudostelligera
Cyclotella radiosa
Cyclotella schumannii
Melosira varians
Skeletonema potamos
Stephanodiscus cf. *binderanus*
Stephanodiscus hantzschii
Stephanodiscus medius
Stephanodiscus minutulus
Stephanodiscus neoastreae
Stephanodiscus parvus
Thalassiosira sp.
Thalassiosira visurgis
Thalassiosira weissflogi
Pennales
Achnanthes biasoletiana
Achnanthes clevei
Achnanthes conspicua
Achnanthes exigua
Achnanthes hungarica
Achnanthes laevis
Achnanthes lanceolata
Achnanthes lanceolata ssp. *dubia*
Achnanthes lanceolata ssp. *frequentissima*
Achnanthes lanceolata ssp. *frequentissima* var. *rostratiformis*
Achnanthes minutissima
Achnanthes ploenensis
Amphora inariensis
Amphora libyca
Amphora montana
Amphora ovalis

Amphora pediculus
Amphora sp.
Amphora veneta
Asterionella formosa
Bacillaria paradoxa
Caloneis amphisbaena
Caloneis bacillum
Caloneis silicula
Caloneis sp.
Cocconeis pediculus
Cocconeis placentula
Craticula accomoda
Cymatopleura elliptica
Cymatopleura solea
Cymbella affinis
Cymbella amphicephala
Cymbella caespitosa
Cymbella cistula
Cymbella helvetica
Cymbella lanceolata
Cymbella microcephala
Cymbella minuta
Cymbella prostrata
Cymbella silesiaca
Cymbella sinuata
Cymbella tumida
Denticula tenuis
Diatoma ehrenbergii
Diatoma mesodon
Diatoma moniliformis
Diatoma vulgare
Diatoma vulgare, morphotyp capitulata
Diploneis ovalis
Diploneis sp.
Epithemia sp.
Fragilaria arcus
Fragilaria brevistriata
Fragilaria capucina
Fragilaria capucina var. *gracilis*
Fragilaria capucina var. *rumpens*
Fragilaria capucina var. *vaucheriae*
Fragilaria construens
Fragilaria crotonensis
Fragilaria fasciculata
Fragilaria leptostauron
Fragilaria parasitica var. *parasitica*
Fragilaria parasitica var. *subconstricta*
Fragilaria pinnata
Fragilaria ulna var. *acus*
Fragilaria ulna var. *ulna*
Frustulia vulgaris
Gomphonema angustum
Gomphonema augur
Gomphonema gracile
Gomphonema micropus
Gomphonema minutum
Gomphonema olivaceum var. *olivaceum*
Gomphonema parvulum
Gomphonema sp.
Gomphonema tergestinum
Gomphonema truncatum
Gyrosigma acuminatum
Gyrosigma attenuatum
Gyrosigma scalproides
Hantzschia amphioxys
Meridion circulare
Navicula atomus var. *atomus*
Navicula atomus var. *permitis*
Navicula bacillum
Navicula capitata
Navicula capitata var. *lueneburgensis*
Navicula capitatoradiata
Navicula cari
Navicula confervacea – cain forming
Navicula contenta
Navicula costulata
Navicula cryptocephala
Navicula cryptotenella
Navicula cuspidata
Navicula decussis
Navicula erifuga
Navicula gallica var. *perpusilla*
Navicula gastrum
Navicula goeppertiana
Navicula gregaria
Navicula integra
Navicula lanceolata
Navicula meniscus var. *grunowii*
Navicula meniscus var. *meniscus*
Navicula minima
Navicula minuscula
Navicula oblonga
Navicula placentula
Navicula protracta
Navicula pupula
Navicula pygmaea
Navicula radiosa
Navicula recens
Navicula reichardtiana
Navicula reinhardtii
Navicula rhynchocephala
Navicula salinarum
Navicula schroeterii
Navicula seminulum
Navicula slesvicensis
Navicula splendula
Navicula ssp.
Navicula subhamulata
Navicula subminuscula
Navicula tenelloides
Navicula tripunctata
Navicula trivialis
Navicula veneta
Navicula viridula var. *rostellata*
Navicula viridula var. *viridula*
Neidium dubium
Neidium sp.
Nitzschia acicularis
Nitzschia amphibia
Nitzschia angustata
Nitzschia angustata
Nitzschia calida
Nitzschia capitellata
Nitzschia clausii
Nitzschia constricta
Nitzschia debilis
Nitzschia dissipata var. *dissipata*
Nitzschia dubia
Nitzschia fonticola
Nitzschia fruticosa
Nitzschia graciliformis
Nitzschia graciliformis
Nitzschia gracilis
Nitzschia heufferiana
Nitzschia hungarica
Nitzschia inconspicua
Nitzschia intermedia
Nitzschia levidensis
Nitzschia linearis
Nitzschia linearis var. *subtilis*
Nitzschia microcephala
Nitzschia palea var. *palea*

Nitzschia paleacea
Nitzschia recta
Nitzschia sigmoidea
Nitzschia sinuata var. *delognei*
Nitzschia sociabilis
Nitzschia spp.
Nitzschia sublinearis
Nitzschia tryblionella
Nitzschia tubicola
Pinnularia borealis
Pinnularia major
Pleurosira laevis f. *laevis*
Rhoicosphenia abbreviata
Surirella angusta
Surirella brebissonii
Surirella crumena
Surirella linearis var. *helvetica*
Surirella minuta
Surirella sp.
Tabellaria flocculosa

Chlorophyta

Volvocales

Chlamydomonas braunii
Chlamydomonas monadina
Chlamydomonas sp. (elongated)
Chlamydomonas sp. (ovoid)
Pandorina morum
Phacotus sp.

Pteromonas aculeata

Chlorococcales

Actinastrum hantzschii
Ankyra lanceolata
Ankistrodesmus gracilis
Chlorococcum spp.
Chodatella quadriseta
Closteriopsis limneticum
Coelastrum astroideum
Coelastrum microporum
Coenococcus planktonicus
Crucigenia tetrapedia
Crucigeniella apiculata
Crucigeniella rectangularis
Dictyosphaerium ehrenbergianum
Kirchneriella lunaris
Lagerheimia genevensis
Lagerheimia longiseta
Micractinium pusillum
Monoraphidium contortum

Monoraphidium griffithii
Monoraphidium markovae
Monoraphidium minutum
Oocystis lacustris
Oocystis marssonii
Pediastrum boryanum
Pediastrum duplex var. *duplex*
Pediastrum duplex var. *gracillimum*
Pediastrum simplex var. *simplex*
Pediastrum simplex var. *echinulatum*
Pediastrum tetras
Scenedesmus acuminatus elongatus
Scenedesmus armatus
Scenedesmus brevispina
Scenedesmus denticulatus
Scenedesmus dispar
Scenedesmus ecornis
Scenedesmus intermedius
Scenedesmus obtusus
Scenedesmus opoliensis
Scenedesmus protuberans
Scenedesmus quadricauda large
Scenedesmus quadricauda small
Scenedesmus quadrispina
Scenedesmus spinosus
Scenedesmus acuminatus
Scenedesmus acutus var. *globosus*
Scenedesmus ecornis disciformis
Schroederia setigera
Tetrademus major
Tetraedron caudatum
Tetraedron minimum
Tetraselmis cordiformis
Tetrastrum staurogeniaeforme
Tetrastrum sp.
Ulothricales
Elakatothrix sp.
Gloeotila sp.
Koliella longiseta
Zygnematales
Spirogyra sp.
Desmidiiales
Closterium acutum var. *linea*
Closterium acutum
Closterium moniliferum
Cosmarium sp.
Staurostrum cingulum
Staurostrum paradoxum

3.4 Number of taxa, biovolume and biomass

The longitudinal variation in the number of taxa in the River Danube is shown in Fig. 10A. A maximum number of 100 taxa is observed at Backa Palanka (HR, RS, JDS45, rkm 1300). The minimum of 51 taxa occurs at Dunaföldvár (HU, JDS35, rkm 1560). On average, 72 taxa are observed.

The variation of phytoplankton fresh-weight biomass in the river and the main tributaries is presented in Fig. 10B. Biomass in the Danube ranges from 0.15 mg L⁻¹ at JDS 1 upstream of Iller, rkm 2600 to 6.96 mg L⁻¹ at JDS 46, upstream of Novi Sad, rkm 162. Biomass concentration remains at low levels in the upstream and downstream section of the Danube. Values higher than 2 mg L⁻¹ algal biomass occur between Baja (HU, rkm 1481) and Grocka (RS, rkm 1132). These concentration thresholds are reached or slightly exceeded at certain points further downstream, e.g. upstream of Cernavoda, near Braila and in the Sulina canal, all in RO. Highest concentrations of around 6.5 mg L⁻¹ biomass are reached in the Novi Sad/Tisa confluence region between rkm 1262 and rkm 1200. The thin line in Fig. 10B indicates Diatom contribution ranging from 30 to 95% with an average of 82%. Biomass input from the larger tributaries to the river Danube is highly variable from very low values in e.g. the Inn and Jantra to high contributions

from e.g. the Morava, Velika Morava or Timok (Fig. 10B, bars). Longitudinal variation in phytoplankton fresh-weight biomass is similar to the fluctuations in chlorophyll-a. Both variables are significantly correlated ($r^2 = 0.95$, $n = 100$, Fig. 11). The number of taxa is weakly correlated to total biomass ($r^2 = 0.31$, $n = 75$). Based on data from Katlin Zsuga, both phytoplankton biomass and chlorophyll-a are significantly correlated with total zooplankton abundance ($r^2 = 0.42$, $n = 73$, $p < 0.001$). Phytoplankton biomass and relative abundance data of the tributaries are summarized in Annex C

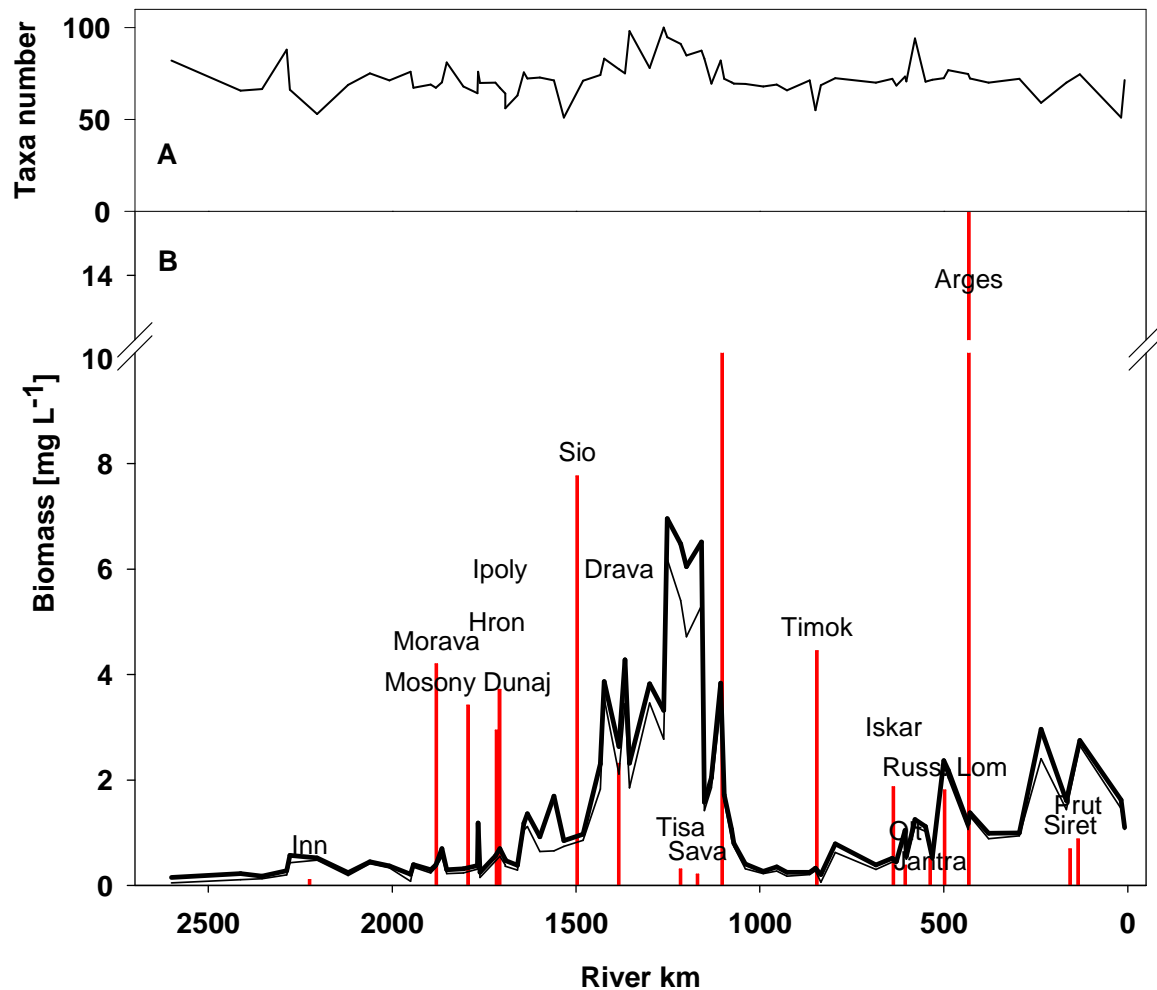


Fig. 10 Development of phytoplankton biomass (B) in mg L⁻¹ along the River Danube (black line) and input from the major tributaries (red bars). The thin line is the contribution by diatoms.

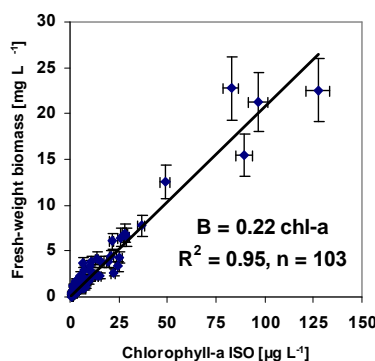


Fig. 11 Relation of fresh-weight biomass to ISO-derived chlorophyll-a. The equation and the coefficient of determination are inserted. The correlation is significant at the $p < 0.001$ level.

Centric diatoms generally dominate in the phytoplankton of the Danube. The main taxa identified in the Danube were Thalassiosiraceae (*Cyclotella*, *Cyclostephanos*, *Stephanodiscus* and *Thalassiosira spp.*). Their relative abundance varies between 4.6 % at Oberloiben (A, JDS10, rkm 2008) and 96.9 % at Vilova, Kilia arm (RO, UA, JDS 93: rkm 18) with an average of 68.4 %.

Although three distinct sections have been identified during JDS2 (see above), number of taxa, species composition, concentration of chlorophyll-a and biomass are described here for the nine geomorphologic reaches of the Danube proposed during JDS1 for comparison.

REACH 1: NEU-ULM (JDS 1) – PASSAU (JDS 5)

The biomass of phytoplankton estimated during JDS2 increases from 0.15 mg L⁻¹ upstream of the Iller to 0.57 mg L⁻¹ at Niederalteich (DE, rkm 2278), upstream of the confluence with the Inn. Chlorophyll-a concentration ranges from a local maximum of 3.63 µg L⁻¹ upstream of the Iller to 1.68 at Niederalteich. The number of phytoplankton taxa found in Reach 1 varied from 66 -88 (mean 47). The relative abundance of centric diatoms ranges from 13.3% to 62.3% without any obvious trend, similar to the Cryptomonads which vary from 13.3 to 23.9%.

REACH 2: JOCHENSTEIN (JDS 7) – HAINBURG (JDS 14)

Downstream of the confluence with the River Inn, characterized by high inorganic turbidity, phytoplankton biomass decreases to values between 0.3 and 0.52 mg L⁻¹ with an average of 0.4 mg L⁻¹. Chlorophyll-a concentration increases from 1.12 µg L⁻¹ near Jochenstein (AT, rkm 2204) to 2.23 µg L⁻¹ at Hainburg (AT, rkm 1881). The number of phytoplankton taxa in this Reach is 53 to 75 (mean 68). The relative contribution of centric diatoms varied from 4.6 to 53.9 % (average 23.2 %). Although centric diatoms are relatively low, Bacillariophyceae dominate the reach with a relative biomass of 38 to 92%. Cryptomonads are particularly abundant with 55% of total biomass at Greifenstein (AT, rkm 1950).

REACH 3: BRATISLAVA (JDS16) to Medvedov (JDS 18)

Phytoplankton biomass (0.7 mg L⁻¹) is relatively high at Bratislava probably as a consequence of the input from the Morava, dropping to 0.3 mg L⁻¹ in the Gabčíkovo Reservoir. Chlorophyll-a concentrations are 1.69 and 0.84 µg L⁻¹ respectively. The number of phytoplankton taxa found in this Reach varied from 68 - 81. The relative abundance of the centric diatoms decreased from 70% to 46%.

REACH 4: KOMAROM (JDS 20) – UPSTREAM BUDAPEST (JDS 29)

Biomass values range from 0.4 to 0.7 mg L⁻¹ with a mean of 0.6 mg L⁻¹. Highest concentrations occur below the confluence with the tributaries Hron and Ipoly. Chlorophyll-a concentration gradually increases in the river from 1.12 to 3.63 µg L⁻¹. An average of 67 (range 56-76) phytoplankton taxa is found at the sampling sites of this Reach. The relative abundance of diatoms decreases from 82.1 to 76.7% while green algae reached an increase in relative contribution from 8.6% to 14.0%.

REACH 5: DOWNSTREAM BUDAPEST (JDS 32) – BELGRADE (JDS 50)

This is the reach with maximum biomass increase from 0.9 mg L⁻¹ below Budapest to the overall peak concentration of 7.0 mg L⁻¹ upstream of Novi Sad (RS, JDS 46, rkm 1262). The mean for this reach is 4.7 mg L⁻¹. Similarly, chlorophyll-a concentrations increase from 4.19 to 27.92 µg L⁻¹, again upstream of Novi Sad. Both biomass and chlorophyll-a remain at high level until Belgrade. The section of the Danube between Budapest and Belgrade is that part of the river where phytoplankton development was optimal during the investigation period of JDS2. Oxygen is super-saturated here up to 114% indicating positive photosynthetic activity. With 100 taxa at Backa Palanka (HR, RS, JDS 45, rkm 1300), the highest number of taxa in the plankton is observed in this reach (range 51 –100, mean 80). Centric diatoms dominate the plankton in this stretch ranging from 61 to 87%. Total diatom contribution varies from 38.9 to 91.3%.

REACH 6: UPSTREAM PANCEVO (JDS 52) – IRON GATE RESERVOIR (JDS 62)

Biomass in this reach decreases from 2.1 mg L⁻¹ downstream of Pancevo (RS, JDS53, rkm 1151) to 0.2 mg L⁻¹ in the Iron Gate reservoir at Tekija/Orsova (RS, RO, JDS 62, rkm 954). Concomitantly, chlorophyll-a declines from 11.5 to 0.84 µg L⁻¹ and taxa in the plankton steadily decrease from 83 to 66, mean 72. Centric diatoms are the dominant phytoplankton group; their proportion relative to total biomass

varies between 61.1 and 86.7 % (average 76.3 %). The relative abundance of the Cryptophyta increases from 1.9 to 17.4 % indicating a greater presence in the less turbulent reservoirs. Chlorophyta became less important again.

REACH 7: VRIBICA/SIMIJA (JDS 63) – DOWNSTREAM ZIMNICEA/SVISTOV (JDS 77)

The biomass of phytoplankton ranged from 0.2 (JDS 65), upstream of the Timok to 1.3 mg L⁻¹ at JDS 78, downstream of the Olt. Average biomass is 0.6 mg L⁻¹. The highest transparency of 1.65 m is observed in the Danube in the Iron Gate II (RS, RO, JDS64, rkm 865). Chlorophyll-a concentration varies between 1.2 in the Iron Gate Reservoir II and 14.9 µg L⁻¹ (JDS 75: downstream Olt). The number of phytoplankton taxa found in this reach varies from 55 to 94 (mean 71). Centric diatoms are a main component of the algal plankton (79% - 87%, mean 78.1%).

REACH 8: D/S JATNRA (JDS 82) – RENI (JDS 95)

The biomass of phytoplankton varies between 1.2 mg L⁻¹ downstream of Ruse/Giurgiu (BG, RP, JDS 82, rkm 488) and 3.0 mg L⁻¹ (JDS 87, rkm 295, Upstream Cernavoda) with an average of 1.8 mg L⁻¹.

Correspondingly, chlorophyll-a concentrations range from 1.97 to 10.61 µg L⁻¹ at the same stations.

Between 51 and 77 taxa appear here. Centric diatoms again dominated the phytoplankton; their share varies between 80% and 95%.

REACH 9: DANUBE DELTA (JDS 93-96)

Small variations between 1.0 and 1.7 mg L⁻¹ of phytoplankton biomass occur in the delta arms. Highest chlorophyll-a concentration of 9.1 µg L⁻¹ is found in the Sulina canal at rkm 36, while only 4.3 µg L⁻¹ occur at rkm 94 in the St. Gheorge arm. The Kilia arm is in between. The phytoplankton was dominated by centric diatoms (77 –97%).

3.5 Tributaries and Side-arms of the Danube (see Fig. 8A)

The biomass and composition of phytoplankton in the tributaries and side arms is often similar to the structural characteristics of the main river but deviates in some cases considerably from the plankton of the Danube.

With 0.11 mg L⁻¹, the biomass is small in the River **Inn** (AT, JDS6, rkm 2235). Chlorophyll-a is comparatively high, 1.68 µg L⁻¹ resulting in a relative chl-a content of 1.5%. Only 47 taxa are found in this turbid inflow. diatoms dominate the biomass with 78.6%. Cryptophyta are an important component contributing 20.1%. A 1% share of Cyanoprokaryota must be mentioned.

High phytoplankton biomass and chlorophyll-a is observed in the **Morava**, 4.2 mg L⁻¹ and 13.4 µg L⁻¹ respectively (chl-a content 0.3%). High contributions of Chlorococcal green-algae (32.1%) characterize this tributary (AT, SK, JDS15, rkm 1880). The relative abundance of diatoms is 58.3% almost entirely composed by centric species. The Morava carries the highest load of suspended particles (TSS = 114.8 mg L⁻¹) of all the tributaries visited. Samples from the upstream stations MO1 and MO2 were not analyzed or not available.

The next two tributaries, the rivers **Hron** (HU, JDS24, rkm 1716) and **Ipoly** (SK, HU, JDS25, rkm 1708) are very similar in biomass and chlorophyll-a (2.9 and 3.7 mg L⁻¹ biomass, 7.3 and 6.7 µg L⁻¹ chl-a). The composition of the plankton in both streams is dominated by diatoms, 70.2 and 50.1% respectively, largely centric species. Cyanoprokaryotes contribute 1.2 and 0.8%. With 19.7% Cryptophyta are relatively abundant in the River Ipoly.

The Hungarian river **Sio** (JDS37, rkm 1497) is exceptionally rich in Euglenophytes (77.2%). All other groups are of minor importance. Biomass is 7.8 mg L⁻¹, equivalent to 36.6 µg L⁻¹ chl-a (content 0.5%). Plankton in the mouth of the River **Drava** (HR, JDS42, rkm 1382) mimics autumn lake plankton. The 2.3 mg L⁻¹ biomass are dominated to 91% by diatoms, largely species from the class Pennales. The concentration of chl-a is 11.5 µg L⁻¹. The resulting chl-a content of the biomass is 0.5%. The amount of total-P is 0.6 mg L⁻¹. At upstream station Drava 1, chlorophyll-a is 3.4 µg L⁻¹ and biomass 0.7 mg L⁻¹ composed of 65% diatoms, 24.5% green algae and 11.5% Crpytophyceae.

At the confluence with the Danube, the River **Tisa** (RS, JDS49, rkm 1216) contains 0.3 mg L⁻¹ biomass and 2 µg L⁻¹ chl-a (chl-a content 0.6%). The biomass consists of 66% diatoms, largely centrics. The 11.2 % contribution from Dinoflagellates is the second largest among the tributaries. The share of the

Cryptophytes is 18.5% which is similar to the findings in the River Ipoly. The 2.7% Cyanoprokaryotes are worth mentioning. The upstream stations Tisa 2 and Tisa 3 have chl-a and biomass concentrations of 5.6 and 5.0 $\mu\text{g L}^{-1}$, and 1.1 and 1.0 mg L^{-1} respectively. Composition of phytoplankton was similar in both cases: both diatoms and green algae have shares of around 35% and Cryptophytes near 30%. Samples from stations Tisa 1 and Tisa 4-6 were not available.

In Belgrade, biomass concentration in the River **Sava** (SR, JDS51, rkm 1170) is 0.2 mg L^{-1} and has a corresponding chlorophyll-a level of 1.7 $\mu\text{g L}^{-1}$. The phytoplankton is composed of 53% diatoms, largely centric species, 14% Cryptophytes and 2.2% Cyanoprokaryotes. With 21%, the contribution from Euglenophytes is rather high. The rest are Chlorophytes. The Sava has the highest visibility of all the tributaries, Secchi-depth is 1.05 m. Upstream samples from the Sava were not available.

The third inflow on the Serbian territory, the **Velika Morava** (SR, JDS56, rkm 1103) is rich in both biomass (12.5 mg L^{-1}) and chl-a (48.9 $\mu\text{g L}^{-1}$). Diatoms contribute 84% to total biomass, exclusively centric species. Other components of significance are the Chlorophytes with 8.3% and again the Euglenophytes with 7%. The three upstream samples VM1, VM2 and VM3 taken by the national team are very rich in chlorophyll a, 96.6, 82.6, and 127 $\mu\text{g L}^{-1}$ respectively. The corresponding biomass values are 21.2, 22.6, and 22.6 mg L^{-1} . Contribution of the algal groups in VM1 is 56.2% diatoms, 33.4 green algae and 10.4% Cryptophyceans. At station Velika Morava 2 composition is similar (63.3, 24.6 and 12.1%) and at VM3 the corresponding relative abundance data are 60.8, 30.1 and 9.0%.

The **Timok** river on the Serbian-Bulgarian border (JDS66, rkm 845) is dominated to 95.3% by diatoms, entirely centrics. The rest is made up from Cryptophytes, 3.6% and green-algae, 1.1%. Biomass is similar to the Morava, 4.4 mg L^{-1} and chl-a is 21.2 $\mu\text{g L}^{-1}$. The oxygen saturation of 128% in the Timok is the greatest super-saturation found in all the inflows.

The **Iskar** river (BG, JDS71, rkm 637) has a concentration of 1.9 mg L^{-1} fresh-weight biomass and 6.6 mg L^{-1} chl-a. The plankton is composed to 73.9% by diatoms of which 88% are centric species. In addition, 20.5% Chlorophytes and 4.7% Cyanoprokaryotes are present. Chlorophyll-a concentrations at the upstream stations Iskar 1 and Iskar 2 are 1.7 and 7.8 $\mu\text{g L}^{-1}$. Biomass has not been evaluated.

Compared to the Iskar, the biomass of phytoplankton and the chlorophyll-a concentrations in the **Olt** River (RO, JDS 74, rkm 605), 0.4 mg L^{-1} and 1.7 $\mu\text{g L}^{-1}$ respectively, are low. Similar to observations during JDS1, this river is rich in Dinophyta-species, 31.9%, the highest contribution in any of the tributaries. Green algae share 24.7%, centric diatoms 20.4%, Cryptophyta 12%, and Cyanoprokaryotes 10.6%. Density of total suspended solids is 42.4 mg L^{-1} of which 87% are inorganic. Two upstream samples were collected by the national team (Olt1 and Olt2). Station Olt1 has only 1.4 $\mu\text{g L}^{-1}$ chl-a, consisting of 57.1% diatoms, 34.0% Chlorophyta and 8.9% Cryptophyta. Biomass has not been analyzed at Olt1. At station Olt2, biomass is 1.6 mg L^{-1} and chl-a 4.5 $\mu\text{g L}^{-1}$. The station is characterized by a 32.6% share of Cryptophyceans, almost equal to the 37.5% diatoms. Green algae present about 30%.

The 12% SRP contained in the total-P concentration of 0.6 mg L^{-1} in the **Jantra** River (BG, JDS78, rkm 537) produces 0.5 mg L^{-1} biomass and a surprisingly low 0.6 $\mu\text{g L}^{-1}$ chl-a. The resulting chl-a content is therefore as low as 0.1% indicating low pigmented cells. Most likely this is a reflection of the large 78.7% contribution from Euglenophytes which are accompanied by 16.6% Cyanoprokaryotes. The samples from stations Jantra1 and Jantra2 contain 0.3 and 2.0 $\mu\text{g L}^{-1}$ chlorophyll-a. Composition and biomass has not been evaluated for these samples.

In the **Russenski Lom** River (BG, JDS 81, rkm 498), 1.2 mg L^{-1} Despite this exceptional availability of inorganic phosphorus, chlorophyll-a reaches only 8.4 $\mu\text{g L}^{-1}$ and biomass concentration is 1.8 mg L^{-1} , possibly an effect of high turbidity (81.6 mg L^{-1}). Plankton composition consists of 61.3% Euglenophytes and 19.5% Cyanoprokaryotes. All other groups share less than 10%. The upstream stations in Russenski Lom (RL1 and RL2) have chlorophyll-a values of 8.9 and 12.3 $\mu\text{g L}^{-1}$ with 50 and 61% contribution from Chlorophyta probably including Euglenophytes not differentiated by the DFS measurements. diatoms in the two samples are 48.2 and 34.3% respectively. Cyanoprokaryota contribute 4.7% at RL2. Biomass data are not available for these stations.

The **Arges** River in Romania (JDS84, rkm 432) is the most polluted stream analyzed. Despite a Secchi-depth of 0.1 m and an oxygen saturation of 17%, both the lowest values observed anywhere, 15.5 mg L^{-1} biomass and 89.3 $\mu\text{g L}^{-1}$ chl-a are produced. Different species of the colonial Cyanoprokaryote genus

Microcystis, mainly *M. aeruginosa*, account for 99.7% of the biomass. Compared to the confluent station, the two Arges stations upstream contain surprisingly little chlorophyll-a ($2.8 \mu\text{g L}^{-1}$ at Arges1 and $5.6 \mu\text{g L}^{-1}$ at Arges2). Algal group composition and biomass could not be analyzed.

In the **Siret River** (RO, JDS90, rkm 157), phytoplankton chlorophyll-a amounts to $2.8 \mu\text{g L}^{-1}$ and biomass is 0.7 mg L^{-1} . The assemblage is composed of 75.2% diatoms of which about half are centrics, 9.9% Dinophyta, 7.8% Cryptophyta, and 6.7% Chlorophyta.

Values in the River **Prut** on the border between Romania and Moldavia (JDS81, rkm 135) are similar to those in the Siret but contribution of Cryptophyta and Chlorophyta are higher, 23.9 and 15.9% respectively while diatoms account for 60.2%. of which 75% are centric species. Two upstream stations are available for the River Prut (P1 and P2). The chlorophyll-a values for these two stations are $2.2 \mu\text{g L}^{-1}$ and $3.4 \mu\text{g L}^{-1}$ respectively, corresponding to biomass of 1.0 mg L^{-1} and 1.1 mg L^{-1} . Station P1 is composed of 42.6% diatoms, 30.4% Cryptophyceans and 30% green algae while P2 has only 0.6% Cryptophyceans but a much higher share of Chlorophytes, 60.9%.

The two examples from the side arms of the Danube are both situated in Hungary. The 3.4 mg L^{-1} biomass in the **Moson Danube arm** (JDS19, rkm 1794) is dominated to 80.8% by diatoms, mainly species of the Centrales. Concentration of chl-a is $10.4 \mu\text{g L}^{-1}$. Although the Secchi disk visibility is 1.1 m in the **Szentendre side arm** (JDS28, rkm 1892) both biomass and chl-a are much lower than in the Moson Danube, 0.3 mg L^{-1} and $1.7 \mu\text{g L}^{-1}$ respectively.

In the tributaries and side arms, both chlorophyll-a and biomass are significantly correlated to SRP ($\text{PO}_4\text{-P}$) concentrations, $r^2 = 0.47$ and 0.36 respectively ($n=19$, $p<0.001$). Phytoplankton biomass and relative abundance data of the tributaries are summarized in Annex C.

3.6 FRR-fluorometry, photosynthetic activity and primary productivity

When phytoplankton is in a dark adapted state, e.g. during night or when the light is weak, all reaction centers are in an active, open state and the fluorescence yield is minimal. In this state, fluorescence is at a baseline value F_0 . When all the traps are closed the maximum fluorescence level (F_m) is reached. Variable fluorescence is obtained by subtracting F_0 from F_m ($F_v = F_m - F_0$). The potential yield of the photochemical reaction is therefore given by F_v/F_m , which is quantitatively related to the photochemical efficiency of PSII (BUTLER 1972).

Theoretically, the **baseline fluorescence (F_0)** should be related to the chlorophyll content of the sample. In fact, fluorescence baseline signals in the River Danube correlate significantly ($n = 75$, $p<0.001$) with all types of chlorophyll-a estimates. The coefficient of determination, r^2 is 0.62, 0.68, and 0.78 for ISO chl-a, DFK and DFS derived chl-a respectively.

The **photochemical efficiency of PSII (F_v/F_m)** remains within typical values (average 0.53, range 0.4 - 1.0) for most of the entire Danube (Fig. 12A). Higher values peaking at 1 occur at the Novi Sad/Tisa confluence region between Batina (rkm 1424) and Grocka (rkm 1132), coinciding with the pattern of Chl-a and biomass, which reached values higher than $10 \mu\text{g L}^{-1}$ chl-a or 2 mg L^{-1} algal biomass in this region. Rates of F_v/F_m are highest when biomass is sufficiently large, discharge moderate and under-water light conditions acceptable. In the downstream section of the Danube until the outflow to the Black sea, F_v/F_m values are again low ranging from 0.35 to 0.65, average 0.49.

The **functional absorption cross section (σPSII)** is rather uniform with an average of 499, range 321 - 757 (Fig. 12B). The river plankton, frequently moving through the vertical light gradient of the water column, acclimate its photosynthetic apparatus to the prevailing environmental conditions. As a consequence, the distribution of σPSII will be rather uniform (e.g. MOORE et al 2003) but significantly decreases along the river corridor ($r^2 = 0.61$, $n = 75$, $p<0.001$). Slow flowing, impounded or artificially deepened river stretches may favor a kind of 'stratification', where phytoplankton cells can acclimate to the light regime. Generally, observations on σPSII can be interpreted by the light history of the cells (KOLBER et al. 1988, 1990). Non-photochemical quenching can cause a reduction of σPSII up to 50% during a day (FALKOWSKI et al. 1994, OLAIZOLA et al. 1994). Photoacclimation over a longer period

on the other hand can cause changes of σ_{PSII} by a factor of 3 (KOLBER et al. 1988). Moreover, there is variability in σ_{PSII} due to species composition (KOLBER et al. 1988). Lower values of σ_{PSII} are described during the mixing period in Lakes, when diatom populations dominate the phytoplankton assemblages (MOORE et al. 2003, KAIBLINGER and DOKULIL 2006). The nutrient status of the cells also influences σ_{PSII} . Studies of BERGES et al. (1996) have shown higher σ_{PSII} following nutrient limitation. In the case of the Danube, nutrient limitation may be of minor importance, as SRP was always available in sustainable amounts. The regulatory factor is far more for light availability which is rather low because of the high amount of suspended solids in most stretches of the Danube.

Typical for diatom dominated phytoplankton, the optical absorption cross section decreases with the increase of cellular pigmentation and pigment packaging during adaptation to low light conditions, hand in hand with a higher light utilization efficiency (BRACHER and WIENCKE 2000). Under light limited conditions, the maximum quantum yield of charge separation has been reported to reach values of 0.07–0.09 (GREENE et al. 1994, BABIN et al. 1995, ARBONES et al. 1995) which is in accordance with our findings. The nutrient status also affects the optical absorption cross section of phytoplankton because it is directly related to the synthesis of components of the light harvesting apparatus.

Photosynthetic rates (PR) calculated from these fluorescence parameters represent **potential primary production (PPP)** because single samples are measured on board in the dark and not several in the *in situ* light gradient. Values characterize near surface production. Results are biased because measurements were performed for logistic reasons at different times of the day and hence different light acclimation of the assemblages. The final outcome of the exercise shall therefore be interpreted with utmost caution.

In general PPP rates remain low in the upper reach of the Danube (Fig. 12C). Peaks at Niederalteich (DE, JDS5, rkm 2278), Greifenstein (AT, JDS11, rkm 1950) and in the upstream Budapest region (rkm 1692 – 1658) can simply be a reflection of mid-day measurements and acclimation to the previous light history. Rates are rapidly increasing and declining between Batina (HR, RS, JDS40, rkm 1424) and Grocka (RS, JDS54, rkm 1132), largely corresponding with the wax and wane of both chlorophyll-a and plankton biomass (Fig. 12C). Maximum production rate, $132.9 \text{ mg C m}^{-3} \text{ h}^{-1}$ is reached upstream of Novi Sad (RS, JDS 46, rkm 1262). Further downstream values remain low except for a single peak of $20.8 \text{ mg C m}^{-3} \text{ h}^{-1}$ in the Iron Gate II Reservoir (RS, RO, JDS64, rkm 865). The average hourly production rate in the river is $10.8 \text{ mg C m}^{-3} \text{ h}^{-1}$. Potential production ranges from a minimum of 0.013 in the Sulina arm (RO, JDS95, rkm 36), most likely affected by the high turbidity resulting from TSS, to the maximum at Novi Sad mentioned above. The median is $3.5 \text{ mg C m}^{-3} \text{ h}^{-1}$.

Not all tributaries were measured. Production in the mouth of the major inflowing streams is generally low except for the Rivers Hron and Ipoly, and the Szentendre side arm which reach 37.3 , 23.7 and $12.4 \text{ mg C m}^{-3} \text{ h}^{-1}$ (Fig. 12C, red bars). All other tributaries have much lower production values. The average rate for all tributaries is $6.7 \text{ mg C m}^{-3} \text{ h}^{-1}$ (range of $0.03 - 37.3$, median 1.9).

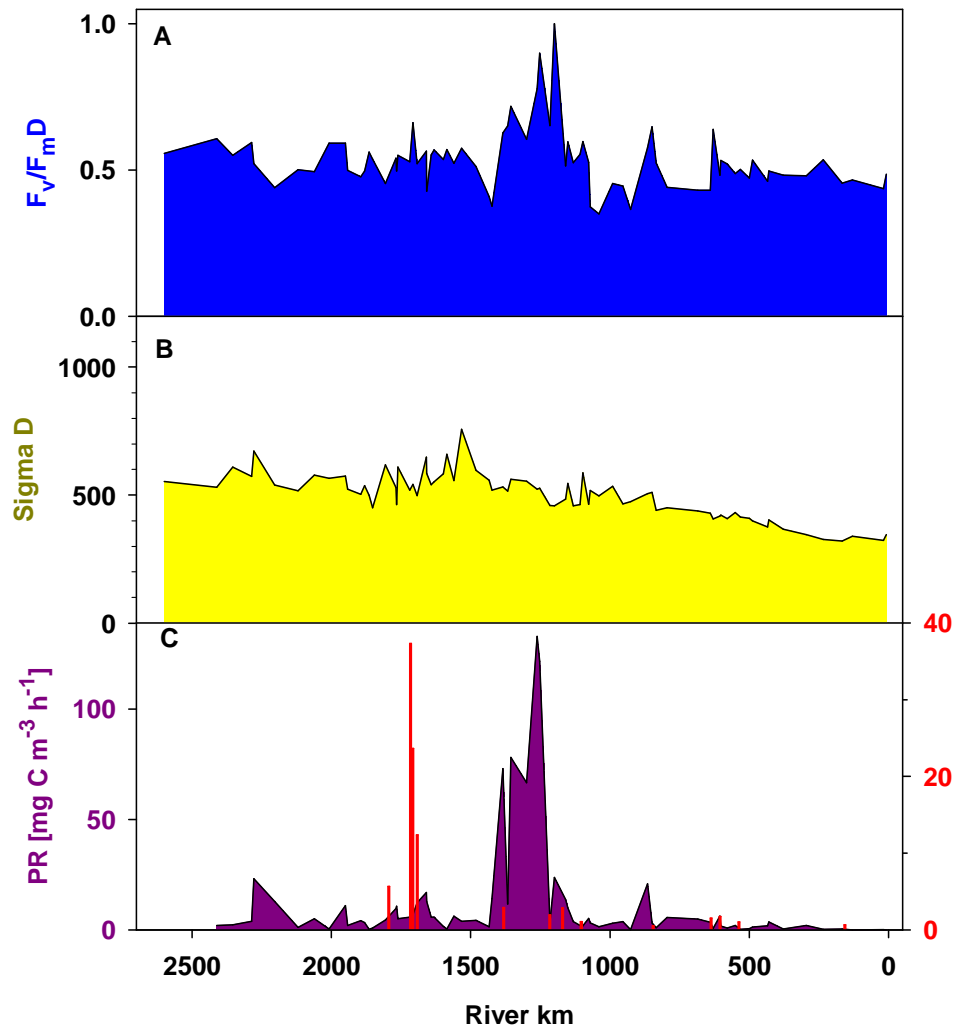


Fig. 12 Photosynthetic parameters. A. F_v/F_m - variable fluorescence, B. ΣD - functional absorption cross-section, C. Photosynthetic rate (PR) calculated from these parameters for the river (dark pink area) and the tributaries (red bars). Note the different scale on the right hand y-axis.

4 Water quality estimates

Assessment of water quality according to the Water Framework Directive (WFD) requires at least four sampling dates per year. One measurement is therefore insufficient and non-conclusive for classification using phytoplankton. Nevertheless, a first attempt is made here to assess water quality.

Chlorophyll-a concentrations are converted to quality classes using the MLIM-Expert Group system which was also used for the Trans-National Monitoring Network (TNMN). In this system, the continuum of chlorophyll concentrations is divided into five classes, of which class II represents the quality objective of the WFD (Table 6).

Table 6 Quality class and corresponding chlorophyll-a level according to TNMN.

Quality Class	I	II	III	IV	V
Chlorophyll-a ($\mu\text{g L}^{-1}$)	25	50	100	250	>250

According to this classification, most chlorophyll-a values fall into quality class I ($<25 \mu\text{g L}^{-1}$). Values of water quality class II are observed at rkm 1384, upstream Drava and in the Novi Sad region and downstream of Tisa between rkm 1262-1200. From the tributaries, 15 streams are below $25 \mu\text{g L}^{-1}$ chl-a. Rivers Sio and Velika Morava, 36.6 and $48.9 \mu\text{g L}^{-1}$ respectively, qualify in class II while the Arges ($89.3 \mu\text{g L}^{-1}$) must be ascribed to class III. River phytoplankton is largely characterized by centric diatoms while tributaries are very rich in species diversity.

An other way to assess the water quality in the River Danube and its tributaries is to adopt preliminarily the type specific WFD criteria developed for a large variety of running waters including large rivers in Germany (MISCHKE et al. 2005, MISCHKE and BEHRENDT 2005). In this case however, extreme caution is necessary for several reasons:

1. The criteria are not specifically designed for the River Danube although data from the Danube were incorporated in the large data set
2. The metrics should be average values calculated from at least four observations per year. We use data from only one observation!
3. The critical levels of the variables must be discussed especially for TP!
4. No attempt is made to calculate trophic indices from indicator taxa because there is still uncertainty which taxa to use and different levels of taxonomic resolution within the centric diatoms.
5. From the set of metrics developed in Germany, only a sub-set is used here

The type specific class boundaries for total phosphorus (TP) and Chlorophyll-a for large rivers from MISCHKE and BEHRENDT (2005) are summarized in Table 7

Table 7 Type-specific levels of total phosphorus (TP) and chlorophyll-a (Chl-a) for the WFD metric ‘pre-degradation according to trophic level’ proposed for large rivers in Germany from MISCHKE and BEHRENDT (2005).

Metric	Quality class	TP [$\mu\text{g L}^{-1}$]	Chl-a [$\mu\text{g L}^{-1}$]
1	High	< 50	< 10
2	Good	50-150	10-20
3	Moderate	150-200	20-30
4	Poor	200-300	30-50
5	Bad	> 300	> 50

Assessment based on chlorophyll-a for the upper reach of the Danube till rkm 1500 (confluence with the River Sio) indicates **high status** and consequently belongs to quality class 1 (Fig. 13). The next two stations, rkm 1481, Baja and rkm 1434, Hercegszanto are in **good status**. At Batina, rkm 1424 und 1384 upstream of the inflow of the River Drava water quality is assessed as **moderate**. Downstream of the Drava, water quality returns to **good** possibly an effect of dilution (rkm 1367 and 1355, Dalj). The following 100 km of river stretch from rkm 1300 to rkm 1200 show water quality characteristics which must be qualified as **moderate**. Thereafter, water quality first improves to **good** till rkm 1132, Grocka and then returns to **high** for the rest of the river until the Black Sea is reached. The boundary between high and good is only slightly exceeded at rkm 295, upstream of Cernavoda and at rkm 167, near Braila. Assessment of chlorophyll-a concentrations in the tributaries and side arms result in the following picture: The water quality in the River Arges is **bad**, in the rivers Sio and Velika Morava it is **poor** and in the River Timok water quality is **moderate**. All other tributaries and side arms qualify into **good or high**.

Trying to assess the TP-concentrations as they are given by VITUKI, all values except two out-liers qualify the Danube as **good** (not shown here). This contradicts the situation especially in the middle reach and all other biological parameters there.

The calculation of two additional metrics, the Pennales-metric and the Chlorophyte-metric (not shown here) give somewhat inconclusive results or are difficult to interpret at present. The Pennales-metric is designed to show degradation to class 3 when contribution to total biomass drops below 20%. Similarly, the Chlorophyte-metric should represent degradation when green algal contribution rises above 5%. Both metric have to be checked carefully for their usefulness in large rivers such as the Danube.

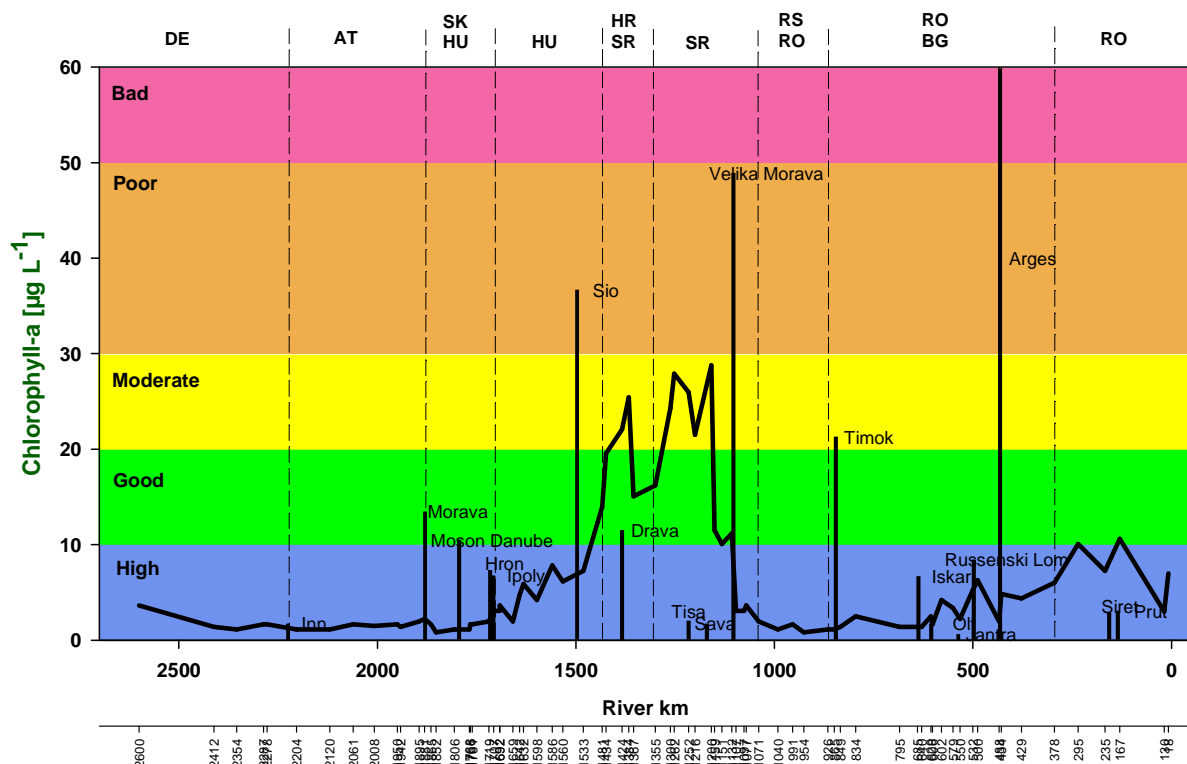


Fig. 13 Assessment of the water quality in the River Danube and the tributaries using the metric chlorophyll-a according to the preliminary method of MISCHKE and BEHRENDT (2005)

5 Summary and Conclusions

During the JDS2 expedition, 327 algal taxa are identified in the plankton of the Danube and its major tributaries which is more than during JDS1. Basically the increase is due to a more detailed analysis of the diatoms often contributing a large number of benthic species to the plankton. The phytoplankton of the river Danube is dominated by diatoms, mainly centric species from the genera *Cyclotella*, *Cyclostephanos*, *Stephanodiscus* and *Thalassiosira* spp.

From the distribution of phytoplankton chlorophyll-a and biomass along the river corridor, three reaches can be defined: An upstream reach from upstream Iller to Baja with chlorophyll-a values below $10 \mu\text{g L}^{-1}$ and biomass concentrations below 2 mg L^{-1} (rkm 2600 – 1481), a middle reach where values exceed this threshold from downstream Baja to Grocka (rkm 1481 – 1132) and a downstream reach with generally

low values again. Maximum values of both parameters have decreased by about 5x compared to results from JDS1. Chlorophyll content of phytoplankton biomass varies from 0.1 – 0.84% with an average of 0.45%.

Basically, all quantitative phytoplankton variables are much lower than during JDS1. This might be partly a result of the different hydrological conditions but must also to a large extent be attributed to better sewage treatment. The high trophic potential, based on phosphorus concentrations both total and inorganic, is only realized in the middle reach of the Danube. Compared to the situation found during JDS1 the peak of chlorophyll and biomass has moved downstream from Dunaföldvár in Hungary to near Novi Sad in Serbia.

Statistical analysis indicates close relation between the longitudinal variation of chlorophyll-a concentration and the fluctuation of phytoplankton biomass values which in turn is related to the abundance of zooplankton. To some extent, phytoplankton biomass is also related to the variation in the number of taxa present.

The biomass and composition of phytoplankton in the side-arms of the Danube is similar to the structural characteristics in the river. In the tributaries, highest values of phytoplankton biomass/chl-a concentrations are found in several tributaries where the eutrophic status was usually underlined by high nutrient concentrations. The most polluted river is the Arges.

Assessment of water quality according to the Water Framework Directive (WFD) requires at least four sampling dates per year. One measurement is therefore insufficient and non-conclusive for classification using phytoplankton. First assessment results however, indicate high to good water quality except for the middle reach.

It must be emphasized however, that direct comparison of chemical and biological concentrations of the two investigation periods might be inconclusive because of the different hydrological discharge situations. The smaller concentrations during JDS2 can partly be a reflection of dilution due to higher run-off. Comparison could certainly be improved by calculation of total load from discharge data for both periods.

6 Recommendations

As it turns out from the comparison of JDS1 and JDS2, expeditions or cruises such as the Joint Danube Surveys are important sources of information but are just snap-shots of water quality at one particular period of the year. We would highly recommend appointing national teams in each country which monitor the river and the main tributaries regularly at least four times per year. In addition, automatic monitoring stations should be installed, at least one per country, to obtain high frequency data of important variables. Considering the taxonomic complexity of most samples and the high back-ground turbidity making quantification by the Utermöhl-technique difficult, we would recommend to adopt alternative strategies. For the taxonomic evaluation, qualitative samples shall be taken (10 µm net), split into sub-samples and sent to specialists for proper determination similar to the practice with zoobenthos samples. Instead of the time consuming and imprecise counting of very turbid samples, it might be recommended to use ISO chlorophyll-a as a measure of plankton biomass. Fluorescence instruments which allow the estimation of both chl-a and the more important algal groups can be used in addition. Quantification of algal species might then be done in the samples simply applying scores from 1-5.

Based on the experience on frozen and transported chl-a samples, we suggest to perform the extraction and analysis of chl-a according to the ISO standard immediately on board of the ship.

7 Acknowledgments

We appreciate very much the generous help and the good company of the core team members and both crews of the research ships Argus and Szèchenyi during the cruise. The good relationship with the organizing team of the ICPDR is kindly acknowledged. We thank Adriana Danielopol for laboratory analysis of the algal pigments and Judith Römer for the preparation and evaluation of the diatom samples. This work would not have been possible without the good cooperation with the Federal Agency for Water Management and their Institute for Water Quality, Austria which also financed the trip (contract No. 410-7/2007). We are particularly grateful to Dr. Rodinger for providing a field microscope and for various

other supports. Last but not least, we would like to thank the DWS Hydro-Ecology GmbH, which handled the contract, for the very good and long lasting cooperation.

8 References used for algal identification

- BARTA, Z., FELFÖLDY, L., HAJDU, L., HORVÁTH, K., KISS, K., SCHMDT, A., TAMÁS, G., UHERKVICH, G. & VÖRÖS, L. 1976:** A zöldalgák (Chlorococcales) rendjének kishatározója. Vízügyi Hidrobiológia 4, 343pp., Budapest, ISBN 963 602053 1.
- BOURRELLY, P. 1966:** Les algues d'eau douce. Tome I. Les algues vertes. 1-511. - N.Boubée et Cie, Paris.
- BOURRELLY, P. 1968:** Les algues d'eau douce. Tome II. Les algues jaunes et brunes. Chrysophycées, Phéophycées et Diatomées. 1-438. - N. Boubée et Cie, Paris.
- BOURRELLY, P. 1970:** Les algues d'eau douce. Tome III. Les algues bleues et rouges. Les Eugléniens, Peridiniens et Cryptomonadines. 1-512. - N. Boubée et Cie, Paris.
- COMPERE, P. 1989 :** Flore pratique des algues d'eau douce de Belgique 2. Pyrrophytes, Raphidophytes, Euglenophytes, Jardin Botanique National de Belgique, Meise, 208pp.
- COX, E.J. 1996:** Identification of freshwater diatoms from live material, Chapman & Hall, London, 158pp.
- ETTL, H. 1978:** Xanthophyceae. 1. Teil. Süßwasserflora von Mitteleuropa. 3, 1-530. - Gustav Fischer Verlag, Stuttgart, New York.
- ETTL, H. 1983:** Chlorophyta I. Phytomonadina. Süßwasserflora von Mitteleuropa. 9, 1-807. - Gustav Fischer Verlag, Stuttgart, New York.
- FELFÖLDY L. 1972:** A kékalgák (Cyanophyta) kishatározója. - Vízügyi Hidrobiológia, 1, 1-257. VIZDOK, Budapest.
- FELFÖLDY L. 1981:** A zöldalgák Desmidiáles rendjének kishatározója. - Vízügyi Hidrobiológia, 10, 1-276. VIZDOK, Budapest.
- FELFÖLDY L. 1985:** A zöldalgák Phytomonadina csoportjának kishatározója. - Vízügyi Hidrobiológia, 14, 1-161. VGI, Budapest.
- GRIGORSZKY I., VASAS F., BORICS G. 1999:** A páncélos-ostoros algák (Dinophyta) kishatározója. - Vízi Természet-és Környezetvédelem, 8, 1-220. KGI, Budapest.
- KOMAREK, J. & FOTT, B. 1983:** Chlorophyceae (Grünalgen). Ordnung: Chlorococcales. In: Huber Pestalozzi, G. (ed.), Das Phytopankton des Süßwassers, Reihe 'Die Binnengewässer' XVI, 7 (1), 1044S., Schweizerbart, Stuttgart, ISBN 3-510-40023-2
- HARTLEY, B. 1996:** An atlas of British diatoms based on illustrations by H.G. Barber and J.R. Carter, ed. P.A.Sims, Biopress, Bristol, 601pp.
- HINDÁK, F., 1977:** Studies on the Chlorococcal algae (*Chlorophyceae*) I, Biologické Práce XXIII/4, Slovak Academy of Sciences, Bratislava, 190 pp.
- HINDÁK, F., 1980:** Studies on the Chlorococcal algae (*Chlorophyceae*) II, Biologické Práce XXVI/6, Slovak Academy of Sciences, Bratislava, 195 pp.
- HINDÁK, F., 1980:** Studies on the Chlorococcal algae (*Chlorophyceae*) II, Biologické Práce XXVI/6, Slovak Academy of Sciences, Bratislava, 195 pp.
- HINDÁK, F., 1984:** Studies on the Chlorococcal algae (*Chlorophyceae*) III, Biologické Práce XXX/1, Slovak Academy of Sciences, Bratislava, 308 pp.
- HINDÁK, F., 1988:** Studies on the Chlorococcal algae (*Chlorophyceae*) IV, Biologické Práce XXXIV/1-2, Slovak Academy of Sciences, Bratislava, 263 pp.
- HINDÁK, F., 1990:** Studies on the Chlorococcal algae (*Chlorophyceae*) V, Biologické Práce XXVI, Slovak Academy of Sciences, Bratislava, 225 pp.
- HINDÁK, F., 1996:** Klúč na určovanie nerozkonárených vláknitých zelených rias (Ulotrichineae, Ulotrichales, Chlorophyceae). Key to the unbrached filamentous green algae ((Ulotrichineae, Ulotrichales, Chlorophyceae), Bulletin Slovenskej botanickej spoločnosti pri SAV Supl. 1, 77pp., ISBN 80-967292-2-5.

- HUBER-PESTALOZZI, G. 1950:** Cryptophyceen, Chloromonadinen, Peridineen. Das Phytoplankton des Süßwassers. 3. Teil. In: Thienemann A. (ed.): Die Binnengewässer, 16,3, 1-310. - E. Schweizerbart'sche Verlagsbuchhandlung (Nägele u. Obermiller), Stuttgart.
- HUBER-PESTALOZZI, G. 1955:** Euglenophyceen. Das Phytoplankton des Süßwassers. 4 Teil. In: Thienemann A. (ed.): Die Binnengewässer, 16, 4, 1-606. - E. Schweizerbart'sche Verlagsbuchhandlung (Nägele u. Obermiller), Stuttgart.
- JAVORNICKY, P. 1976:** Minute species of the genus *Rhodomonas* KARSTEN (Cryptophyceae). - Arch. Protistenkunde, 118, 98-106.
- JAVORNICKÝ, P. 2003:** Taxonomic notes on some freshwater planktonic Cryptophyceae based on light microscopy, *Hydrobiologia* 502, 271-283.
- KUSEL-FETZMANN, E. 2002:** Die Eugleophytenflora des Neusiedler Sees, *Abhandlungen der Zoologisch-Botanischen Gesellschaft in Österreich* 32, 1-115.
- KOMÁREK, J., K. ANAGNOSTIDIS 1999:** Cyanoprokariota 1. Teil: Chroococcales. Süßwasserflora von Mitteleuropa, 19/1, 1-548. - Gustav Fischer Verlag, Jena, Stuttgart, Lübeck, Ulm.
- KOMÁREK, J., B. FOTT 1983:** Chlorophyceae (Grünalgen, Ordnung: Chlorococcales). In: Thienemann A. (ed.): Die Binnengewässer, Band 16: Das Phytoplankton des Süßwassers, 7. Teil, 1. Hälfte, 1-1044. - Schweizerbart'sche Verlagsbuchhandlung (Nägele u. Obermiller), Stuttgart.
- KRAMMER, K., H. LANGE-BERTALOT 1986:** Bacillariophyceae. 1. Teil: Naviculaceae. Süßwasserflora von Mitteleuropa, 2/1, 1-876. - Gustav Fischer Verlag, Stuttgart, New York.
- KRAMMER, K., H. LANGE-BERTALOT 1988:** Bacillariophyceae. 2. Teil: Bacillariaceae, Epithemiaceae, Surirelliaceae. Süßwasserflora von Mitteleuropa, 2/2, 1-596. - Gustav Fischer Verlag, Stuttgart, New York.
- KRAMMER, K., H. LANGE-BERTALOT 1991:** Bacillariophyceae. 3. Teil: Centrales, Fragilariaceae, Eunotiaceae. Süßwasserflora von Mitteleuropa, 2/3, 1-576. - Gustav Fischer Verlag, Stuttgart, New York, Jena.
- KRAMMER, K., H. LANGE-BERTALOT 1991a:** Bacillariophyceae. 4. Teil: Achnanthaceae; Kritische Ergänzungen zu *Navicula* (Lineolatae und Gomphonema); Gesamtliteraturverzeichnis Teil 1-4. Süßwasserflora von Mitteleuropa, 2/4, 1-437. - Gustav Fischer Verlag, Stuttgart, Jena.
- MROZINSKA, T. 1985:** Chlorophyta VI. Oedogoniophyceae: Oedogoniales. - Süßwasserflora von Mitteleuropa 14, 1-624. Gustav Fischer Verlag, Stuttgart, New York.
- NÉMETH J. 1997:** Az ostoros algák (Euglenophyta) kishatározója 1. (2. javított és bővített kiadás). [A guide for the identification of Euglenophyta occurring in Hungary, I.] (Second revised and enlarged edition). - *Vízi Természet- és Környezetvédelem* 3, 1-319. KGI, Budapest.
- LENZENWEGER, R. 1996:** Desmidiaceenflora von Österreich, Teil 1, *Bibliotheca Phycologica* 101, Hg.L. Kies & R. Schnetter, J. Cramer, Borntraeger Verlagsbuchhandlung, Berlin, 162S.
- LENZENWEGER, R. 1997:** Desmidiaceenflora von Österreich, Teil 2, *Bibliotheca Phycologica* 102, Hg.L. Kies & R. Schnetter, J. Cramer, Borntraeger Verlagsbuchhandlung, Berlin, 216S.
- LENZENWEGER, R. 1999:** Desmidiaceenflora von Österreich, Teil 3, *Bibliotheca Phycologica* 104, Hg.L. Kies & R. Schnetter, J. Cramer, Borntraeger Verlagsbuchhandlung, Berlin, 218S.
- NAVARINO, G. 2003:** A companion to the identification of cryptomonad flagellates (Cryptophyceae = Cryptomonadea). *Hydrobiologia* 502, 225-270.
- POPOVSKY, J., L. A. PFIESTER 1990:** Dinophyceae (Dinoflagellida). Süßwasserflora von Mitteleuropa, 6, 1-272. - Gustav Fischer Verlag, Jena, Stuttgart.
- UHERKOVICH, G. 1966:** Die Scenedesmus-Arten Ungarns, *Akadémiai Kiadó, Budapest*, 173S.
- WOTOWSKI, K. & HINDÁK, F. 2005:** Atlas of Euglenophytes, *VEDA, Slovak Academy of Sciences*, Bratislava, 126pp.

4.5.9 References general

- ARBONES, B., FIGUEIRAS, F.G. AND VARELA, R. 2000:** Action spectrum and maximum quantum yield of carbon fixation in natural phytoplankton populations: implications for primary production estimates in the ocean. *J Mar Syst* 26: 9-114.

- BABIN, M., THERIAULT, J.C., LEGENDRE, L., NIEKE, B., REUTER, R., AND CONDAL, A. 1995:** Relationship between the maximum quantum yield of carbon fixation and the minimum quantum yield of chlorophyll a in vivo fluorescence in the Gulf of St. Lawrence. *Limnol Oceanogr* 40: 956-968.
- BERGES, J.A., CHARLEBOIS, D.O., MAUZERALL, D.C. AND FALKOWSKI, P.G. 1996:** Differential effects of nitrogen limitation on photosynthetic efficiency in photosystems I and II in microalgae. *Plant Physiol* 110: 689-696.
- BRACHER, A.U. AND WIENCKE, C. 2000:** Simulation of the effects of naturally enhanced UV radiation on photosynthesis of Antarctic phytoplankton. *Mar Ecol Prog Ser.* 196: 127-141.
- BUTLER, W.L. 1972:** On the primary nature of fluorescence yield changes associated with photosynthesis. *Proc. Nat. Acad. Sci. USA.* 69: 3420-3422.
- FALKOWSKI, P.G., GREENE, R. AND KOLBER, Z. 1994:** Light utilization and photoinhibition of photosynthesis in marine phytoplankton. In: Baker NR, Bowyer JR eds *Photoinhibition of photosynthesis: from molecular mechanisms to the field.* Bios scientific publishers, Oxford, p 407-432.
- GEIDER, R.J., GREENE, R.M., KOLBER, Z., MACINTYRE, H.L. AND FALKOWSKI, P.G. 1993:** Fluorescence assessment of the maximum quantum efficiency of photosynthesis in the Western North – Atlantic. *Deep-Sea Res* 40: 1205-1224.
- GERHARDT V. & BODEMER, U. 1998:** Delayed fluorescence spectroscopy: A method for automatic determination of phytoplankton composition of freshwaters and sediment interstitial and of algal composition of benthos. – *Limnologica* 29, 313-322.
- GERHARDT V. & BODEMER, U. 1999:** Chlorophyllbestimmung durch *in vivo* Fluoreszenz. – In: TÜMPLING, W.V. AND G. FRIEDRICH eds. *Methoden der Biologischen Wasseruntersuchung Band 2, Biologische Gewässeruntersuchung*, 35-52, G.Fischer, Jena, Stuttgart, Lübeck, Ulm, ISBN 5-437-35170
- GREENBERG, A.E., CLESCERI, L.S., EATON, A.D. eds. 2005:** *Standard Methods for the Examination of Water and Wastewater*, 21st Edition, American Water Works Association, pp, 1368 ISBN: 0875530478
- GREENE, R.M., KOLBER, Z.S., SWIFT, D.G., TINDALE, N.W. AND FALKOWSKI, P.G. 1994:** Physiological limitation of phytoplankton photosynthesis in the eastern Equatorial Pacific determined from variability in the quantum yield of fluorescence. *Limnol Oceanogr* 39: 1061-1074.
- HILLEBRAND, H., DÜRSELEN, C.-D., KIRSCHTEL, D., POLLINGHER, U. and ZOHARY, T. 1999:** Biovolume calculation for pelagic and benthic microalgae. *Journal of Phycology* 35: 403-424.
- KAIBLINGER, C. AND DOKULIL, M.T. 2006:** Application of Fast Repetition Rate Fluorometry to phytoplankton photosynthetic parameters in freshwaters. *Photosynthesis Research* 88: 19-30
- KOLBER, Z.S. AND FALKOWSKI, P.G. 1993:** Use of active fluorescence to estimate phytoplankton photosynthesis in situ. *Limnol Oceanogr* 38: 1646-1665.
- KOLBER, Z.S., PRASIL, O. AND FALKOWSKI, P.G. 1998:** Measurements of variable chlorophyll fluorescence using fast repetition rate techniques: defining methodology and experimental protocols. *Biochem Biophys Acta* 1367: 88-106.
- KOLBER, Z.S., WYMAN, K.D. AND FALKOWSKI, P.G. 1990:** Natural variability in photosynthetic energy conversion efficiency; a field study in the Gulf of Maine. *Limnol Oceanogr* 35: 72-79.
- KOLBER, Z.S., ZEHR, J. AND FALKOWSKI, P.G. 1988:** Effects of growth irradiance and nitrogen limitation on photosynthetic energy conversion in photosystem II. *Plant Physiol* 88: 923-929.
- KRAUSE, H., HELML, M., GERHARDT, V. AND GEBHARDT, W. 1982:** In vivo measurements of photosynthetically active pigment systems in fresh waters using delayed fluorescence. *Archiv Hydrobiologie, Beihefte Ergebnisse der Limnologie* 16, 47-54
- LUND, J. W. G., KIPLING, C., AND LE CREN, E. D. 1958:** The inverted microscope method of estimating algal numbers and the statistical basis of estimations by counting. *Hydrobiologia* 11: 144-170

- MARGALEF, R. 1960 :** Valeur indicatrice de la composition des pigments du phytoplancton sur la productivité, composition taxonomique et propriétés dynamiques des populations. Rapports et Proces-Verbaux des Reunions XV: 277-281.
- MARGALEF, R. 1964:** Modelos experimentales de poblaciones de fitoplancton: nuevas observaciones sobre pigmentos y fijación de carbono inorgánico. Investigación Pesquera. 26: 195-203.
- MARRA, J. 1997:** Analysis of diel variability in chlorophyll a and particulate attenuation. J. Mar. Res. 55: 767-784.
- MAUZERALL, D. 1972:** Light induced changes in Chlorella, and the primary photoreaction for the production of oxygen. Proc. Nat. Acad. Sci., USA. 69: 119-140.
- MISCHKE, U., BEHRENDT, J. KÖHLER AND OPITZ, D. 2005:** Überarbeiteter Endbericht zum LAWA Vorhaben: Entwicklung eines Bewertungsverfahrens für Fließgewässer mittels Phytoplankton zur Umsetzung der EU-Wasserrahmenrichtlinie. IGB Berlin-Friedrichshagen, 100 S.
- MISCHKE, U. UND BEHRENDT, J. 2005.** Vorschlag zu Bewertung ausgewählter Fließgewässertypen anhand des Phytoplanktons. In: C.K. FELD, S. RÖDINGER, M. SOOMERHÄUSER UND G. FRIEDRICH (Hg.), Typologie, Bewertung, Management von Oberflächengewässern. Stand der Forschung zur Umsetzung der EG-Easserrahmenrichtlinie. Limnologie Aktuell 11, 46-62, Schweizerbart'sche Verlagsbuchhandlung, Stuttgart.
- MOORE, C.M., SUGGETT, D., HOLLIGAN, P.M., SHARPLES, J., ABRAHAM, E.R., LUCAS, M.I., RIPPETH, T.P., FISHER, N.R., SIMPSON, J.H. AND HYDES, D.J. 2003:** Physical controls on phytoplankton physiology and production at a shelf sea front: a fast repetition-rate fluorometer based field study. Mar Ecol Prog Ser 259: 29-45.
- OLAIZOLA, M., LAROCHE, J., KOLBER, Z.S. AND FALKOWSKI, P.G. 1994:** Non photochemical quenching and the diadinoxanthin cycle in a marine diatom. Photosynth Res 41: 357-370.
- PADISÁK J., KRIENITZ L. & SCHEFFLER W. 1999:** Phytoplankton. – In: TÜMPLING, W.V. AND G. FRIEDRICH eds. Methoden der Biologischen Wasseruntersuchung Band 2, Biologische Gewässeruntersuchung, 35-52, G.Fischer, Jena, Stuttgart, Lübeck, Ulm, ISBN 5-437-35170-2
- PARSONS, T.R., MAITA, Y. AND LALLI, C.M. 1984:** A manual of chemical and biological methods for seawater analysis. Pergamon Press, Oxford, 173 pp.
- REYNOLDS, C.S. 1984:** The ecology of freshwater phytoplankton. Cambridge University Press, London, 384pp.
- TRAINOR, F.R., 1998:** Biological aspects of *Scenedesmus* Chlorophyceae – phenotypic plasticity, Nova Hedwigia, Beiheft 117, 1-367.
- UTERMÖHL, H. 1958:** Zur Vervollkommnung der quantitativen Phytoplankton-Methodik. - Mitt. Int. Ver. Limnol., 9, 1-38.

List of Figures

- Fig. 1 Physical variables in the River Danube during JDS2. A. Photosynthetic active radiation (PAR) above the water in units of $\mu\text{mol photons per m}^2$ and second. B. Secchi-depth visibility in meters and the depth of euphotic zone (z_{eu}) in meters (green line). C. Attenuation coefficient (K) in units of \ln per meter..... 7
- Fig. 2 Suspended solids in the River Danube during JDS2. Inorganic suspended solids (ISS) in gray and organic suspended solids (OSS) as dark red area. Total suspended solids (TSS) are the sum of ISS and OSS. For comparison SD in meters is plotted here again as a blow up from Fig. 1B. 8
- Fig. 3 Relation of Secchi-depth (SD) to total suspended solids (TSS). The hyperbolic regression curve, the equation, the number of observations, statistics and the coefficient of determination r^2 is inserted. 8
- Fig. 4 Attenuation coefficient K versus: A. TSS, B. ISS, C. OSS. All in mg L^{-1} in the River Danube during JDS2. Note the different scale on the x-axis in C. The 95% confidence interval of the linear regression and the prediction interval is given as blue and red lines respectively. The linear regression equation, number of observations, statistics and the coefficient of determination r^2 is inserted in each panel. 9
- Fig. 5 A. Euphotic depth (dotted blue line) compared to the water depth of the River Danube light gray area. B. Surface water temperature (SWT), $^{\circ}\text{C}$. C. Dissolved oxygen as % saturation (dashed line = 100%) and ammonia concentration ($\text{NH}_4\text{-N}$, $\mu\text{g L}^{-1}$). C. SRP concentration ($\text{PO}_4\text{-P}$, $\mu\text{g L}^{-1}$) and, for comparison chlorophyll-a concentration as grey line..... 9
- Fig. 6. Longitudinal variation of Chlorophyll-a concentration as $\mu\text{g L}^{-1}$ from delayed fluorescence kinetics (DFK) for the River Danube (green symbols and line), vertical green lines indicate standard deviation and the inlets of the major tributaries (red bars). The tributaries are named. The second x-axis gives the exact river rkm where samples are taken. 11
- Fig. 7. A. Chlorophyll-a concentration from delayed fluorescence kinetics (DFK) related to total chlorophyll-a from ISO analysis both as $\mu\text{g L}^{-1}$ uncorrected for phaeopigments (see text for further explanation). B. Chlorophyll-a from delayed fluorescence spectroscopy (DFS) versus chl-a concentration from ISO-determination..... 12
- Fig. 8 Contribution of the four major algal groups Cyanoprokaryota (cyan), Cryptophyta (grey), Bacillariophyceae (dark red) and Chlorophyta (dark green) to total chlorophyll-a from delayed fluorescence spectroscopy (DFS) for the river (lower panel) and the tributaries (upper panel). 13
- Fig. 9 Longitudinal distribution of pigment-related parameters in the river (continuous lines) and the tributaries (bars). A. Chlorophyll-a concentration of ISO-determinations. B. Phaeopigment concentration from ISO determinations. C. Total Carotenoids estimated from additional wavelength measurements in the extracts (see method section for explanation). D. Pigment ratio E_{430}/E_{665} according to Margalef as a measure of the physiological state (for further explanation see methods and the text). 14
- Fig. 10 Development of phytoplankton biomass (B) in mg L^{-1} along the River Danube (black line) and input from the major tributaries (red bars). The thin line is the contribution by diatoms..... 18

Fig. 11 Relation of fresh-weight biomass to ISO-derived chlorophyll-a. The equation and the coefficient of determination are inserted. The correlation is significant at the $p < 0.001$ level.	18
Fig. 12 Photosynthetic parameters. A. F_v/F_m - variable fluorescence, B. Sigma D - functional absorption cross-section, C. Photosynthetic rate (PR) calculated from these parameters for the river (dark pink area) and the tributaries (red bars). Note the different scale on the right hand y-axis.....	24
Fig. 13 Assessment of the water quality in the River Danube and the tributaries using the metric chlorophyll-a according to the preliminary method of MISCHKE and BEHRENDT (2005).....	26

List of Tables:

Table 1 Acid and alkaline version of Utermöhl's Lugol solution	3
Table 2 Notation of fluorescence–photosynthesis relationship	4
Table 3 Summary of descriptive statistics for physical variables in the River Danube during JDS2.....	6
Table 4 Descriptive statistics for pigment data.....	12
Table 5 List of phytoplankton taxa identified during JDS2	15
Table 6 Quality class and corresponding chlorophyll-a level according to TNMN.	24
Table 7 Type-specific levels of total phosphorus (TP) and chlorophyll-a (Chl-a) for the WFD metric 'trophic stage' proposed for large rivers in Germany (MISCHKE et al. 2005).....	25

List of Annexes:

ANNEX A – Sampling stations

ANNEX B – Plankton Taxa occurrence list

ANNEX C – Total Biomass Table

ANNEX D –Methodology of delayed fluorescence, particularly DFK and DFS

ANNEX E – ISO Chlorophyll and pigment calculation

ANNEX F – Basics of Fluorometry (PAM, FRRF)

ANNEX G –Quantitative phytoplankton analysis